chromatin fibers, thicker fibers which appear in cross section as larger and denser dots, each with diameters of about 40 nm (level 3), could also be observed (Fig.1C, D; Table 1).

Mid acrosome phase spermatids These cells correspond to stages 10 to 12 (Fig.6). The striking features are the elongation of the nuclei which start to assume falciform shape. The anterior region is covered by completely-formed acrosome (Fig.2A). The centriolar apparatus is localized in the implantation fossa contiguous to the electron-dense caudal plate of the nucleus (Fig.2A, B). Towards the end of stage 10 and in stage 11 chromatin fibers increase in size to 50 nm in diameter (level 4), which are distributed chiefly in the subacrosomal area, and in the caudal part close to the dense plaque on the posterior nuclear membrane (Fig.1E, F; Table 1). Besides the difference in diameters, the appearances of these fibers are also drastically different: while level 2 and 3 fibers appear as dot-like which is interpreted to be cross sections of highly convoluted fibers, level 4 appear as thick and straight fibers with long sections appearing even in the thin sections (Fig.1E, F). Some level 4 fibers might also be seen as dot-like feature but with less frequency, which is interpreted to be the cross sections of the straight fibers (Fig.1F). From this appearance we believe that during stage 10 the chromatin fibers begin to change in size as well as conformation; while the first 3 levels of chromatin fibers may be randomly coiled, the 4th level fiber, in addition to becoming thicker, also transform to straight threads which are aligned in long parallel orientation. In stage 11 the nucleus is uniformly filled with level 4 fibers (Fig. 1E, F). The next levels of organization are the highly condensed chromatin fibers appearing as large knobs (level 5) and branching cords (level 6) with the thickness varying from 60-70 nm (Fig.2B, D; Table 1) which start to form in the subacrosomal portion of the nucleus; and this result in the initiation of chromatin condensation in the anterior part of the nuclei in stage 12 (Fig.2A-D). These levels 5 and 6 fibers may achieve their thickness and density as the result of lateral association and coalescence of several level 4 fibers. Interestingly, the width of the anterior part of the nucleus is also substantially reduced, suggesting the

2

possibility that the nuclear tapering occurs as the result of this initial chromatin condensation, while the mid and caudal portions of the nucleus are still filled with level 4 fibers and appear rather wide (Fig.2A, B, F).

Late acrosome phase spermatids These cells correspond to stages 13 and 14 (Fig.6). Level 5 and 6 chromatin fibers could be found throughout the nucleus (Fig.3A-F). And the gradient of chromatin condensation progresses from the anterior part until it covers the whole nucleus. And in some spermatids the anterior half of the nuclei may contain completely dense chromatin.

Maturation phase spermatids These cells correspond to stages 15 to 17 (Fig.6) where the acrosomes are fully developed and cover the anterior two-third of the nuclei. Still attached to posterior end of the acrosome are nuclear rings and manchettes (Fig.4A-E; 5A,B). Gradually, the manchettes disappear by being shed out with the residual cytoplasm. The chromatin in the anterior half of the nucleus of stage 15 becomes almost completely condensed, except for small electron-lucent slits or channels between very thick branching chromatin cords, each about 100 nm in width (level 7) (Fig.4B, D; 5A, B; Table 1) whereas in the posterior half of the nucleus there may still be level 5 and 6 and small amount of level 4 fibers (Fig.4A, B, E). The midpiece of the tail is formed between the manchette (Fig.4F). In stage 16 and 17 the chromatin assumes level 7 organization throughout the nucleus (Fig.5A, B).

Immature spermatozoa These cells correspond to stages 18 and 19, when their chromatin becomes almost completely condensed and electron opaque, except for small circular spots which are widely scattered throughout the nucleus (Fig.5C-F).

## Discussion

Leblond and Clermont (1952) have classified rat spermatids into 19 stages based mainly on the acrosome and tail formations. While many investigators have studied the sequence of replacement of histones by transitional proteins and protamines (Balhorn et

41

al., 1984; Heidaran et al., 1988; Alfonso and Kistler, 1993; Meistrich et al., 1994; Oko et al., 1996) the actual morphometric data concerning the change in the higher orders of chromatin fibers and the pattern of their condensation in various stages of spermatids of rats have still not been reported. In this study we have shown that the nuclei of round spermatids (stages 1-7) have mostly 10 nm-thick chromatin fibers (level 1), and certain amount of 30 nm-thick fibers (level 2), and the latter may also aggregate together to form small heterochromatin blocks. In early acrosome phase spermatids (stages 8-9), the chromatin fibers increase to 40 nm, which is designated as level three. These fibers appear as dense dots in cross-sections which we interpret that they are randomly coiled. In mid-acrosome phase spermatids (stages 10-12), further enlargement of chromatin into 50 nm-thick straight fibers (level 4) which assume more parallel orientation were observed. The size and conformation change of chromatin fibers during these stages of spermatids may be the consequence of the loss of histones including various variants of H1 and other core histones, and/or their replacement by transition proteins (TP) as reported earlier (Bucci et al., 1982; Lennox and Cohen, 1984; Meistrich et al., 1994; Oko et al., 1996). In late acrosome phase spermatids (stage 13-14) chromatin fibers increase in thickness to 60-70 nm, starting from the subscrosomal and spreading to the caudal regions of the nucleus. This initial chromatin condensation may be also brought about by TP proteins which are found to be the prevalent lysine-rich proteins in these stages (Courtens and Loir, 1981; Heidaran et al., 1988; Alfonso and Kistler, 1993; Oko et al., 1996; also see Fig.6). The large chromatin cords in maturation phase spermatids (stages 15-17) have similar appearance as chromatin remaining within the heads of rat spermatozoa after being decondensed with urea-DTT, which appeared as thick branching cords about 100 nm in width linked together by thin zig-zag fibers about 30 nm in diameter (Sobhon et al., 1981). The latter fibers disappeared upon subsequent treatment with micrococcal nuclease. As a result we interpreted that the thick chromatin cords represent the highly packed nucleoprotamines linked together by smaller and loosely packed nucleohistones which could represent the remaining histones in the rat

sperm head; and that these nucleohistone fibers were preferential digested away by micrococcal nuclease. This finding supports the pattern of chromatin condensation in late spermatids where the chromatin fibers gradually increase in size, starting from 50 nm parallel straight fibers in stages 11 and 12 to 90-100 nm branching cords in stages 15 to 17. Such increase in thickness of chromatin cords could be viewed as the lateral or parallel association of neighboring 50 nm fibers which later become coalesced and tightly packed together. This final step of condensation could be brought about by protamines, which have been shown to replace TP proteins in stages 15 to 17 spermatids (Platz et al., 1977; Meistrich et al., 1994; also see Fig.6). The pattern of chromatin condensation in rat spermatids may differ from that proposed for human sperm chromatin, where after histones are replaced by protamines the randomly coiled 30 nm nucleohistone fibers turn into 50-100 nm beaded fibers that may be formed by the packing together of compact toroidal-shaped nucleoprotamine beads (Sobhon et al., 1982; Balhorn et al., 1999; Sobhon et al., 2000).

# **Explanation of Figures**

Figure 1 A, B) Stage 1 rat spermatid, showing the nucleus containing mostly euchromatin which consists of two levels of chromatin fibers: level 1 appear as thin zigzag fibers with the thickness about 10 nm (1), and level 2 appear mostly in cross sections as dense dots about 30 nm in diameter (2). Few blocks of heterochromatin (He) consisting of tight aggregations of 30 nm fibers are also present.

C, D) Stage 9 spermatid, showing elongated nucleus with completely formed acrosome (Ac) at the anterior, nuclear ring (nr) and manchette (ma) in the cytoplasm that becomes localized towards the posterior part of the cell (in C). In D, a few large dense dots about 40 nm in diameter (3), which may represent cross sections of larger chromatin fibers, are present in the subacrosomal area and the anterior part of the nucleus.

E, F) Stage 11 spermatid, showing 50 nm straight fibers interlacing with each other; short straight segments (4) as well as dots (arrows) which represent the cross sections of these fibers could also be observed.

Figure 2 A, B, C, D) Stage 12 spermatid: the anterior part of the nucleus contains thick branching chromatin cords with variable thickness at 60 nm (5) and 70 nm (6), which may represent the higher-ordered structures formed by the lateral aggregation of smaller level 4 fibers. The most anterior part of the nucleus usually contains completely condensed chromatin (in C) while the middle and posterior parts still contain 50 nm straight fibers (4) (in B, D).

E, F) The posterior end of the same nucleus showing the implantation fossa occupied by centriole (ce), manchette (ma) attaching to the nuclear ring (nr) and surrounding the nucleus, and the caudal condensation (cd) on the posterior nuclear membrane.

Figure 3 A, B, C, D) Stage 13 spermatid, showing the coalescence of 50 nm fibers (4) to form chromatin cords of larger sizes at 60 nm (5) and 70 nm (6) which are spreading

throughout the nucleus (in A, C, D). In B, the midpiece of the tail (Mp) is formed from the centriole (ce) in the implantation fossa. Nuclear ring (nr) and manchette (ma) are present on both sides of the nucleus.

- E, F) Stage 14 spermatid, showing the formation of highly electron dense chromatin cords at 70 nm (6) and 90-100 nm (7) throughout the nucleus.
- Figure 4 A, B, C, D, E) Stage 15 spermatid, showing completely condensed chromatin in the anterior part of the nucleus (in A, C), and the presence of branching 90-100 nm chromatin cords (7) in the middle portion (in B, D), while the posterior portion (in E) still contains 70 nm (6), 60 nm (5), and 50 nm (4) fibers.
- F) The midpiece of the tail (Mp) and a group of mitochondria are present between the manchettes (ma).
- Figure 5 A, B) Stage 17 spermatid, showing the highly condensed chromatin throughout the nucleus which still appear as branching cords, each about 90-100 nm thick (7), separated by narrow clefts (arrows) which are completely electronlucent.
- C, D, E, F) Stage 18 (C, D) and stage 19 (E, F) spermatids, showing completely condensed chromatin in all areas of the nucleus, except for very small vacuoles which appear as electronlucent spots (arrows).
- Figure 6 A diagram summarizing the changes in sizes and conformation of chromatin fibers and the pattern of chromatin condensation in correlation with the sequence of replacement of histones, transitional (TP) proteins, and protamines (modified from the original diagram of Leblond and Clermont, 1952).

Figure 2

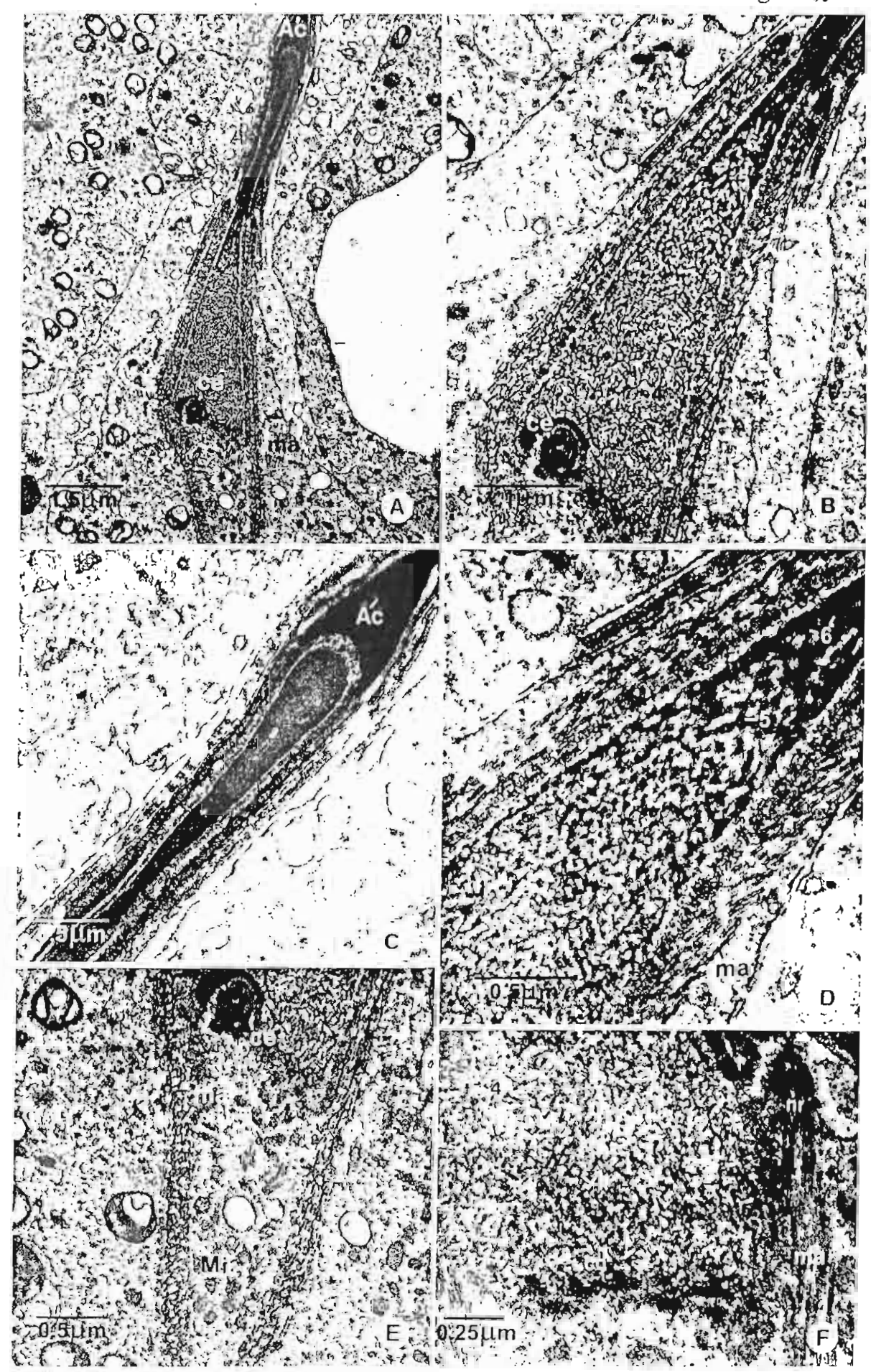


Figure 3

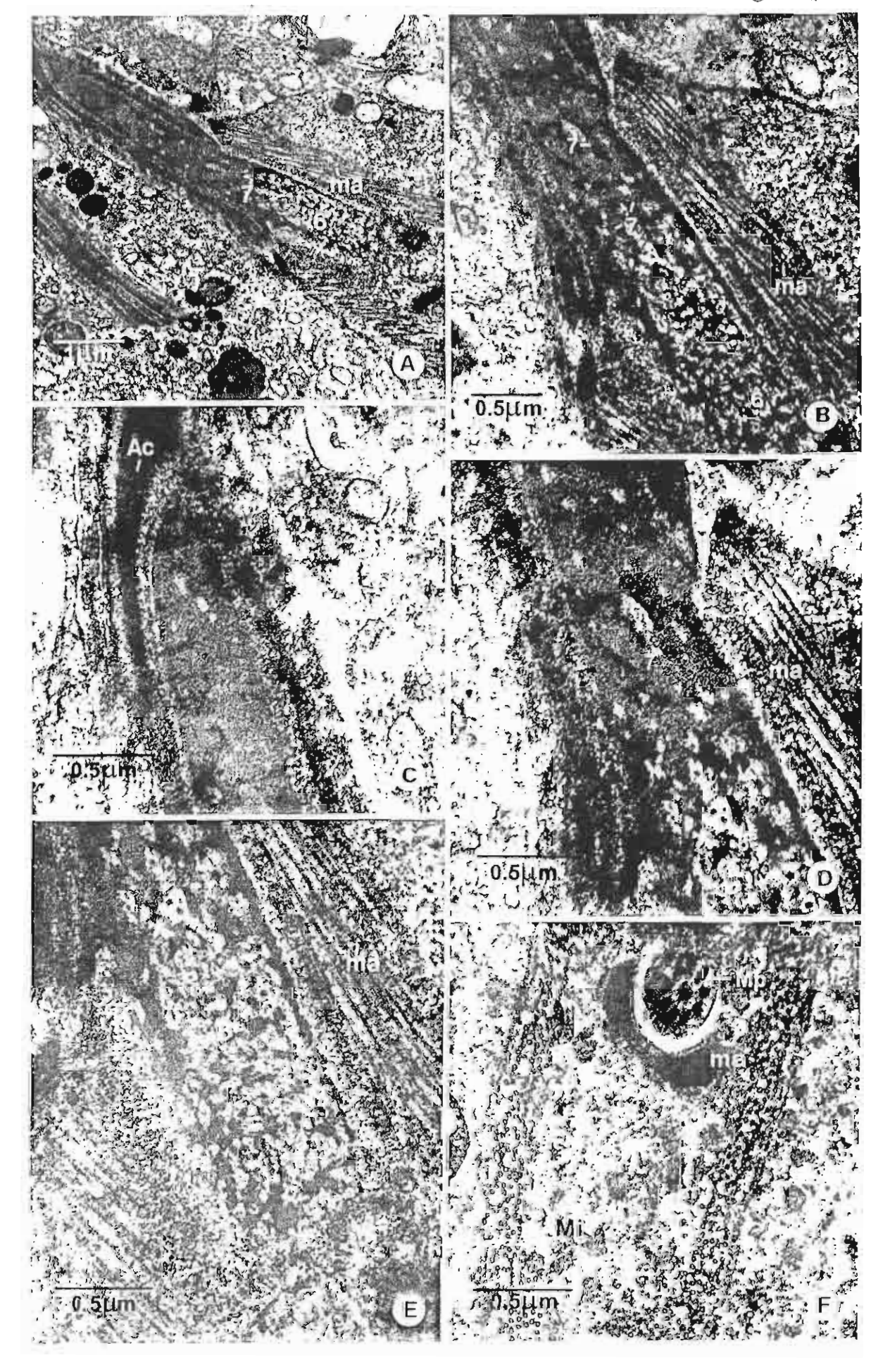


Figure 4

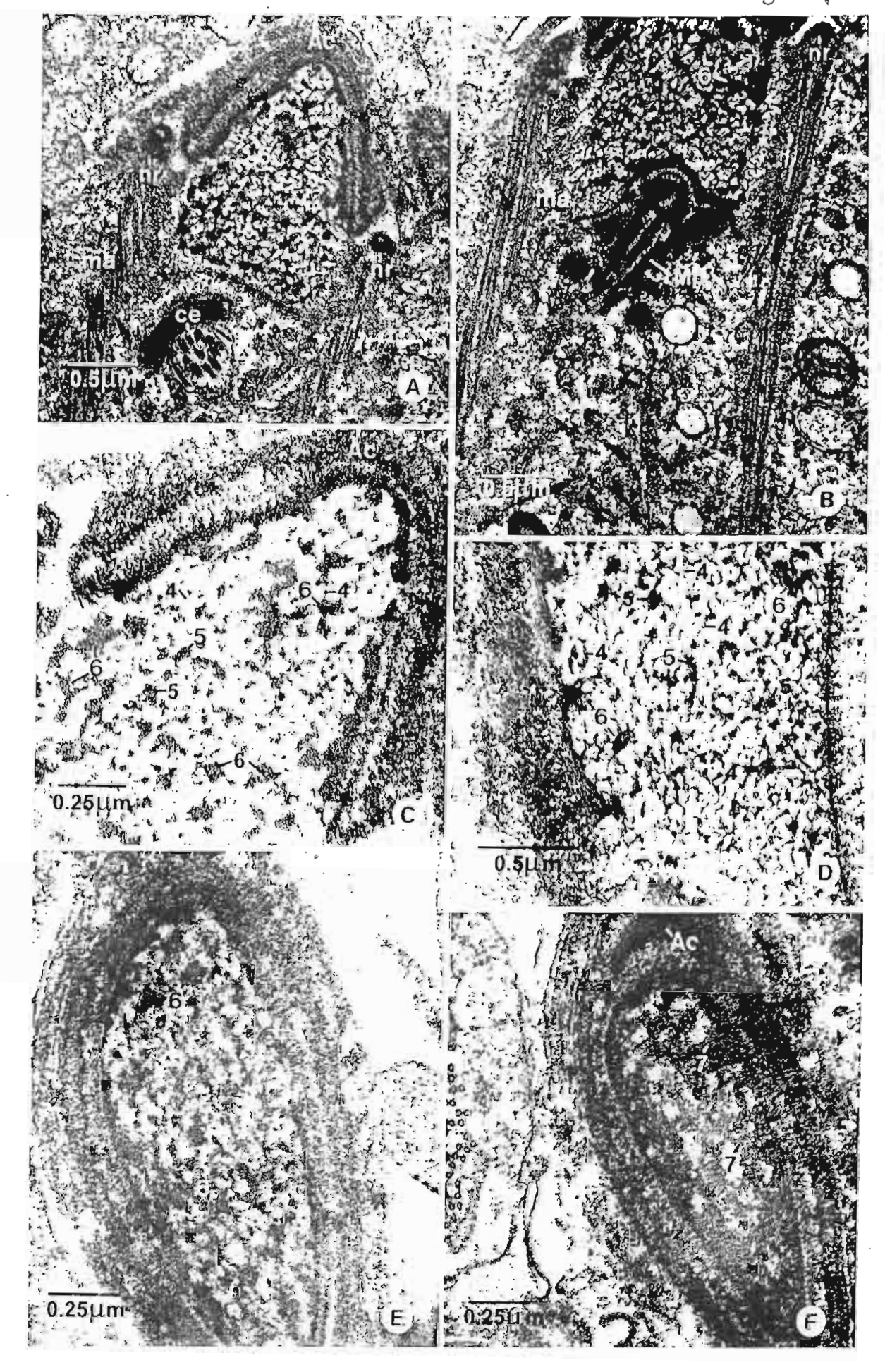
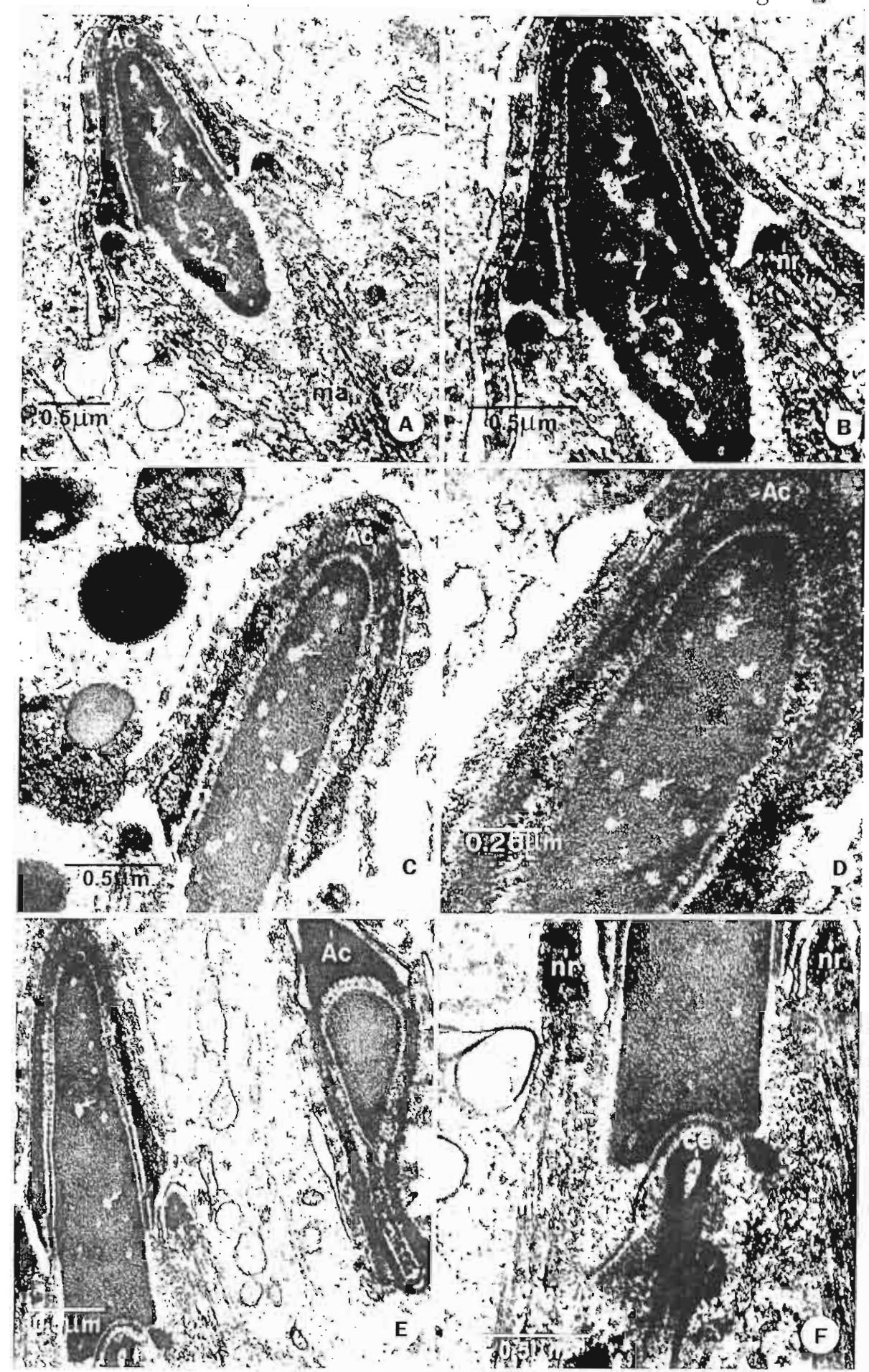


Figure 5



# **Acknowledgement**

This investigation was supported by the Thailand Research Fund (Senior Research Scholar Fellowship to P. Sobhon).

### References

- Alfonso P.J., W.S. Kisler (1993) Immunohistochemical localization of spermatid nuclear transition protein 2 in the testis of rat and mice. Biol Reprod 48: 522-529.
- Balhorn R., Weston S., Thomas C., A. Wyrobek (1984) DNA packaging in mouse spermatids synthesis of protamine variants and four transition proteins. Exp Cell Res 150: 298-308.
- Balhorn R., Cosman M., Thornton K., Krishnan V.V., Corzett M., Bench G., Kramer C.,
  Lee IV J., Hud N.V., Allen M., Prieto M., Meyer-Ilse W., Brown J.T., Kirz J.,
  Zhang X., Bradbury E.M., Maki G., Braun R.E., W. Breed (1999) Protamine
  mediated condensation of DNA in mammalian sperm; in Gagnon, C. (ed): The
  Male Gamete: From Basic Science to Clinical Applications, Cache River Press,
  Vienna, IL pp 55-70.
- Bucci L.R., Brock W.A., M.L. Meistrich (1982) Distribution and synthesis of histone 1 subfractions during spermatogenesis in the rat. Exp Cell Res 140: 111-118.
- Courtens J., M. Loir (1981) A cytochemical study of nuclear changes in boar, bull, goat, mouse, rat and stallion spermatids. J Ultrastruct Res 74: 327-340.
- Dooher G.B., D. Bennett (1973) Fine structural observations on the development of the sperm head in the mouse. Am J Anat 136: 339-361.
- Grimes S.R., P.G. Smart (1985) Change in the stuctural organization of chromatin during spermatogenesis in the rat. Biochim Biophys Acta 824: 128-139.

- Heidaran M.A., Showman R.M., W.S. Kistler (1988) A cytochemical study of the transcriptional and translational regulation of nuclear transition protein 1 (TP1), a major chromosomal protein of mammalian spermatids. J Cell Biol 106: 1427-1433.
- Leblond C.P., Y. Clermont (1952) Definition of the stages of the cycle of the seminiferous epithelium in the rat. Annal New York Academy Sci 55: 548-570.
- Lennox R.W., L.H. Cohen (1984) The alteration in H1 histone complement during mouse spermatogenesis and their significance for H1 subtype function. Dev Biol 103: 80.
- Loir M., M. Lanneau (1984) Structural function of the basic nuclear proteins in ram spermatids. J Ultrastruct Res 86: 262-276.
- Meistrich M.L., Brock W.A., Grimes S.R., Platz R.D., L.S. Hnilica (1978) Nuclear protein transitions during spermatogenesis. Fed Proc 37: 2522-2525.
- Meistrich M.L., Trostle-Weige P.K., M.E.A.B. Van Breek (1994) Separation of specific stages of spermatids from vitamin A-synchronized rat testes for assessment of nucleoprotein changes during spermiogenesis. Biol Reprod 51: 334-344.
- Oko R.J., Jando V., Wagner C.L., Kistler W.S., L.S. Hermo (1996) Chromatin reoganization in rat spermatids during the disappearance of testis-specific histone, H1t, and the appearance of transition protein TP1 and TP2. Biol Reprod 54: 1141-1157.
- Platz R.D., Grimes S.R., Miestrich M.L., L.S. Hnilica (1977) Nuclear protein transitions in rat testis spermatids. Exp Cell Res 110: 31-39.
- Sobhon P., Thungkasemvathana P., N. Tanphaichitr (1981) Electron microscopic studies of rat sperm heads treated with urea, dithiothreitol, and micrococcal nuclease.

  Anat Rec 201: 225-235.
- Sobhon P., Chutatape C., Chalermisarachai P., Vongpayabal V., N. Tanphaichitr (1982)

  Transmission and scanning electron microscopic studies of the human sperm

- chromatin decondensed by micrococcal nuclease and salt. J Exp Zool 221: 61-79.
- Sobhon P, Linthong V, Weerachatyanukul W, Suphamungmee W, Meepol A, Apisawetakan S, Wanichanon C, Sretarugsa P, Chavadej J, Muangmun V Chromatin condensation during spermiogenesis in human. Cells Tissues Organs (submitted).
- Subirana J.A. On the biological role of basic proteins in spermatozoa and during spermiogenesis; in Duckette J.G., P.A. Racey (eds): The Biology of the Male Gamete, Acedemic Press, New York pp 239-244.

STAGES OF MALE GERM			CHROMATIN FIBERS DIAMETERS (nm)	FIBERS DIA	METERS (nm)		
CELLS	Level 1	Level 2	Level 3	Level 4	Level 5	Level 6	Level 7
Golgi & cap phase spermatids (Stages 1-7)	10.01 ± 0.02	30.03 ± 0.13	ı	1	ī.	I	
Early acrosome phase spermatids (Stages 8-9)	$10.03 \pm 0.06$	30.02 ± 0.04	40.03 ± 0.03	ı		ı	i
Mid acrosome phase spermatids (Stages 10-12)	$10.02 \pm 0.05$	30.04 ± 0.04	1	50.01 ± 0.11		-	-1
Late acrosome phase spermatids (Stages 13-14)		,	,	50.05 ± 0.24	61.88 ± 2.50	68.94 ± 1.44	93.13 ± 4.86
Maturation phase spermatids (Stages 15-17)		I DE	1	,		68.39 ± 1.19	94.72 ± 4.48

replaced, while levels 4, 5, 6, 7 are fibers after histones' replacement. At level 4 chromatin fibers significantly increase in size as well as change from coiled to straight conformation. Level 7 is the highest ordered structure when the chromatins appear as branching cords. The measurements of chromatin fibers were Table 1 The sizes of chromatin fibers during condensation in various stages of rat spermatids. Levels 1 and 2 are thought to be fibers before histones are performed in at least 10 cells from each stage.

# veterinary parasitology

An International Journal



Dr. S.M. Taylor 8 Grey Point Helen's Bay Bangor BT19 1LE United Kingdom

Tel: + 44 1247 853331 Fax: + 44 1247 853523

E-mail: stuart\_m.taylor@virgin.net

Editors-in-Chief: S.M. Taylor J.C. Williams

Dr. Prasert Sobhon Dept. of Anatomy Faculty of Science, Mahidol University Rama VI Rd. Bangkok 10400 THAILAND

Vetpar 946

20 October 2001

Dear Dr. Sobhon,

The paper by Dr. A. Sirisriro entitled "Production and characterisation of a monoclonal antibody against recombinant fatty acid binding protein of *Fasciola gigantica* " has been reviewed by the Editorial Panel. It will be acceptable for publication in Veterinary Parasitology subject to some revision. Some of the points requiring attention are marked on the manuscript, and in addition I enclose a copy of one of the reviewer's comments for your further guidance during revision.

Yours sincerely,

S. M. Tienglow

S.M.Taylor

# Veterinary Parasitology

#### REVIEWER EVALUATION SHEET

Manuscript: VETPAR 946

Sirisriro, A., Grams, R., Vichasri-Grams, S., Ardseungneon, P., Pankao, V., Meepool, A., Author(s):

Chaithirayanon, K., Viyanant, V., Tan-Ariya, P., Upatham, E.S. and Sobhon, P.

Production and characterization of a monoclonal antibody against recombinant fatty acid binding protein Title:

of Fasciola gigantica

#### Evaluation

Please encircle the option of your choice and specify your choice below.

This manuscript is acceptable in its present form

This manuscript is acceptable in its present form

This manuscript will be acceptable after minor revision

- This manuscript will be acceptable after moderate revision
  This manuscript will be reconsidered after major revision
- 5. This manuscript is not acceptable for publication
- ......

Comments (Please continue on a separate sheet if more space is needed)

This manuscript looks at the recombinant fatty acid binding protein of Fasciola gigantica. The manuscript is well written, however a bit long for the data presented.

The authors note that the antigens (Page 4 and 5) were dialyzed for 24 hours but neglected to mention what molecular weight cut off membranes were used. What size molecules were allowed to pass out?

Why was the recombinant step necessary? If it was that this was the only way to get enough antigenic . material this should be stated.

The authors experimentally infected mice to get the Schistosome FABP why did they not look at the other logical organism, Fasciola hepatica?

I believe that the manuscript should be reduced in length.

# Title: Production and characterization of a monoclonal antibody against recombinant fatty acid binding protein of Fasciola gigantica

Authors: A. SIRISRIRO<sup>1</sup>, R. GRAMS<sup>4</sup>, S. VICHASRI-GRAMS<sup>2</sup>, P. ARDSEUNGNEON<sup>2</sup>, V. PANKAO<sup>3</sup>, A. MEEPOOL<sup>3</sup>, K. CHAITHIRAYANON<sup>3</sup>, V. VIYANANT<sup>2,4</sup>, P. TAN-ARIYA<sup>1</sup>, E.S. UPATHAM<sup>2</sup> AND P. SOBHON<sup>3</sup>

Affiliations: Departments of <sup>1</sup>Microbiology, <sup>2</sup>Biology and <sup>3</sup>Anatomy, Faculty of Science, Mahidol University, RamaVI Rd., Bangkok, 10400, Thailand.

<sup>4</sup>Faculty of Allied Health Science, Thammasat University, Phahonyothin Rd., Klongluang, Pathumthani, 12120, Thailand.

Short title: Monoclonal antibody to fatty acid binding protein of F. gigantica

Correspondences and reprint request to: Dr. Prasert Sobhon Ph.D.

Department of Anatomy,

Faculty of Science, Mahidol University Rama VI Rd., Bangkok 10400, Thailand

Tel. 662-245-5198

E-mail: scpso@mahidol.ac.th

Fax. 662-247-9880

#### Abstract

In Fasciola parasites fatty acid-binding proteins (FABP) are the carrier proteins that help in the uptake of fatty acids from the hosts' fluids. Attempts have been made to utilize both native and recombinant FABP (rFABP) for immunodiagnosis and vaccine development for fasciolosis. In the present study we have produced a number of monoclonal antibodies (MoAb) against rFABP of Fasciola gigantica. These MoAb were initially screened against rFABP by ELISA and then tested for their specificities by immunoblotting. Five stable clones were selected and characterized further: four of them were of the isotype  $IgG_1$  while one clone was  $IgG_{2a}$ . All the MoAbs reacted with rFABP which has a molecular weight (MW) of 20 kD and with at least two isoforms of native proteins at MW 14.5 kD that were present in the tegumental and crude worm extracts, and the excretion-secretion materials. Immunoperoxidase stainings of frozen sections of adult parasites by using these MoAb as primary antibodies indicated that FABP were present in high concentration in the parenchymal cells and reproductive tissues, in low concentration in the tegument and caccal epithelium. All MoAb crossreacted with a 14.5 kD antigen present in the whole-body extract of Schistosoma mansoni, while no cross reactivities were detected with antigens from Eurytrema pancreaticum and Paramphistomum spp.

Keywords: F. gigantica, fatty acid binding protein, monoclonal antibody, localization

#### Introduction

Trematode parasites are unable to synthesize de novo most of their lipids particularly long chain fatty acids and cholesterol (Meyer et al., 1970). Therefore, they have to depend on fatty acid binding proteins (FABP) for the uptake and transport of these molecules from the host. Phylogenetically, parasite FABPs appear to be related to those appearing in vertebrate tissues including heart, mammary gland, muscle, with about 30% identity of the amino acid level, although no clear functional relationships have been established (Esteves et al., 1997; Moser et al., 1991). Recently, F. hepatica FABP (Fh12) and S. mansoni FABP (Sm15) have been shown to elicit a strong cross protective immunity (Hillyer, 1985; Hillyer et al., 1988a). Mice vaccinated with purified Fh12 prior to challenging with S. mansoni cercariae displayed a 77% reduction in the worm burden (Hillyer et al., 1988b). In addition, Fh12 was found to be expressed in F. hepatica early after the excystment through to the adult stage (Rodriguez-Perez et al., 1992). However, due to the limitation in obtaining sufficient quantity of native FABP as antigen for vaccination, attempts to produce recombinant FABP (rFABP) of F. hepatica (Fh15) have been made. This recombinant protein has been shown to induce a significant level of resistance in hosts to challenges with F. hepatica (Muro et al., 1997) and S. bovis (Abane et al., 2000).

In comparison to *F. hepatica*, there have only been few studies on the cloning and vaccine potential of *F. gigantica* FABP (Estuningsih et al., 1997, Smooker et al., 1997). In the present investigation we have attempted to produce and characterize monoclonal antibodies (MoAb) against recombinant *F. gigantica* FABP. These MoAb were used to immunolocalize FABP in *F. gigantica* tissues, and their cross

reactivities with other trematode parasite antigens were tested in order to probe for their possible applications in immunodiagnosis and vaccine development.

#### Materials and methods

#### Parasite samples

Adult *F. gigantica* were removed from the bile ducts and gall bladders of condemned bovine livers at local slaughterhouses. Other trematode parasites collected from the same group of cattle for a cross reaction study included *Paramphistomum* spp. from the rumen and *Eurytrema pancreaticum* from the pancreas. *S. mansoni* were collected for the cross reaction study from mice infected with cercariae 8 week earlier. All parasite specimens were washed three times with Hank's balanced salt solution (HBS) containing 100 U/ml penicillin and 100 mg/ml streptomycin to remove all traces of blood, bile and contaminating microorganisms.

Excretory-secretory antigens (ES) of adult F. gigantica

The ES-antigens were prepared by incubating freshly collected, living adult parasites in Hank's balanced salt solution (Gibco, USA) at room temperature for 3 hours. The parasite eggs in the culture medium were removed by centrifugation at 5000 g for 20 minutes at 4 °C. The supernatant was dialysed in 0.01M PBS, pH 7.2 at 4 °C for 24 hours, lyophilized, and kept at -20 °C until used.

TA-antigen was obtained by extraction of live adult parasites with 1% Triton X-100 in Tris HCl buffer, pH 8, for 30 minutes at room temperature. The extracting solution was collected and centrifuged at 5000 g for 20 minutes at 4 °C to remove the parasite eggs which may be released during the extraction. The supernatant containing TA-antigen was collected and dialysed in 0.01 M phosphate buffer saline (PBS), pH 7.2 at 4 °C for 24 hours, before it was lyophilized and kept at -20 °C until used.

Whole body antigens (WB) of parasites

Whole adult parasites (*F. gigantica* and other trematodes) were homogenized in 0.01 M PBS, pH 7.2 and then rotated at 4 °C overnight. The suspensions were centrifuged at 5000g, 4 °C, for 20 min and the supernatants were collected and stored at -70 °C until used in subsequent experiments.

The protein contents of all fractions were determined by modified Lowry's method (Lowry et al., 1951).

Preparation of F. gigantica rFABP

A 399 bp cDNA fragment encoding a FABP of *E. gigantica* was cloned by RT-PCR (Grains et al., 2000). The fragment was subsequently cut by *BamH* I and *Sal* I restriction enzymes from pBluescript SK(-) (Stratagene) and subcloned in the bacterial expression vector pQE30 (QIAGEN). The cloning procedure resulted in the addition of 19 amino acids at the N-terminus including a six-residue histidine stretch

for purification. At the C-terminus another 14 amino acids were added to the recombinant FABP. The calculated molecular weight of rFABP is 18.5 kDa. Upon induction by IPTG (1 mM) rFABP was detected by SDS-PAGE analysis in the insoluble protein fraction. It was, therefore, purified by Ni-NTA chromatography under denaturing conditions in 6 M urea following the instructions of the manufacturer (QIAexpressionist, QIAGEN). The eluted protein fractions were analyzed by SDS-PAGE, and FABP-containing fractions were combined and dialyzed against PBS buffer.

Production of monoclonal antibodies (MoAbs) against F. gigantica rFABP

BALB/c mice were immunized subcutaneously with *F. gigantica* rFABP in complete Freund's adjuvant at a dose of 10 µg in 100 µl per mouse. The second injection of a similar dose of the recombinant protein in incomplete Freund's adjuvant was given 3 weeks later. And 20 µg of protein in 100 µl PBS was given intravenously as a final boosting dose 2 weeks later. Hybridomas were produced by fusion of spleen cells from BALB/c mice immunized with *F. gigantica* rFABP and mouse myeloma cells (P3/x63-Ag8). The hybridoma cells that grew successfully in culture were cloned by limiting dilution methods. Only the hybridoma clones that produced high titers of antibodies against rFABP, as screened by indirect ELISA, were selected. Five MoAbs were chosen in this study, namely, 3D4-12, 3D8-1, 3D8-8, 5C5-1 and 6F3-2. The antibody isotypes were determined by ELISA using the Mouse MonoAb-ID kit (ZYMED Laboratories, USA).

Immunoblotting was performed as described previously by Viyanant et al. (1993). Briefly, rFABP, TA, ES, and WB antigens were separated in 12.5% SDS-PAGE and blotted onto a nitrocellulose membrane. As positive controls, the antigenic bands in each fraction were detected by cattle infected sera (CIS) obtained from the pooled sera of naturally infected animals. Strips containing similar antigenic fractions were also screened by MoAbs. For negative controls, the culture fluid (CF) and normal mouse serum (NMS) were used as probes. Cattle antibodies that reacted with the antigenic molecules were detected by peroxidase-conjugated rabbit anti-bovine immunoglobulin, whereas the monoclonal antibody-antigen complexes were detected by peroxidase-conjugated rabbit anti-mouse IgG. The reaction was visualized by further incubation in 3,3 diaminobenzidine (DAB) and H<sub>2</sub>O<sub>2</sub>.

#### Immunolocalization of FABP

The five MoAbs were used for an analysis of the distribution, and relative concentration of FABP in the frozen and acetone-fixed sections of adult *F. gigantica* by immunoperoxidase/DAB staining. Endogenous peroxidase activity was destroyed by pretreating the tissue sections with 3% H<sub>2</sub>O<sub>2</sub>. The positive reaction was demonstrated by Avidin-Biotin-Peroxidase technique as previously described by Viyanant et al. (1993). CIS diluted at 1:50 and 10% fetal calf serum were used as positive and negative controls, respectively.

#### Results

#### Monoclonal Antibodies

Five clones of monoclonal antibodies against rFABP of F. gigantica, namely 3D4-12, 3D8-1, 3D8-8, 5C5-1 and 6F3-2, were produced. Four of them, 3D4-12, 3D8-1, 3D8-8, and 5C5-1 were found to be  $IgG_1$ , while only 6F3-2 was  $IgG_{2a}$ . All monoclonal antibodies were  $\kappa$  light chain. Clone 6F3-2 had the highest titer (up to 2.02 in ELISA OD reading at 492 nm with the cut off point at 0.5).

#### Immunoblotting

The immunoblotting experiment indicated that all MoAbs reacted with a single band of rFABP which has a molecular weight (MW) of 20 kD (Fig.1A). However, when tested against WB TA and ES antigens from adult *F. gigantica*, these MoAbs reacted with native FABP which appeared as a close double band at MW 14.5 kD (Fig. 1B, 2A). When similar antigenic fractions were analysed with polyclonal antibodies against native FABP (kindly given by Dr. Terry Spithill, Monash University, Australia), the identical double band was observed at MW 14.5 (Fig. 2B) which confirmed that the proteins detected by MoAb were FABP. However, in contrast to the MoAb the polyclonal antibodies also reacted with bands in ES and WB at higher molecular weights which could be due to impurities in the native FABP preparation used for immunization.

When tested against WB antigens from three other trematode parasites (S. mansoni, Paramphistomum spp. and Eurytrema pancreaticum), all MoAb showed a

strong cross reaction with a S. mansoni antigen at MW 14.5 kD, while no cross reactions were detected in WB antigens from other parasites (Fig.3).

#### *Immunolocalization*

All MoAbs showed similar immunoperoxidase staining characteristics as represented by MoAb 6F3-2 (Fig.4) which exhibited the strongest reaction. The sites and intensities of the brownish reaction products indicated the location and relative concentration of FABP which were bound to MoAb. The highest intensity was observed in the cytoplasm of parenchymal cells and their processes (Fig. 4A, B, C). However, while most parenchymal cells (Pc<sub>1</sub>) were intensely stained, some parenchymal cells (Pc<sub>2</sub>, Pc<sub>3</sub>) were only moderately or lightly stained (Fig. 4B, C). The testicular and ovarian tissues were also moderately stained with the early stage germ cells on the periphery of the gonadal follicles appeared more intensely stained than the late stage cells in hte center (Fig. 4E, F). The basal part and the surface of tegument were moderately stained (Fig.4B). Most cytoplasm of the caecal epithelium was lightly stained, whilst the apical cytoplasm and lamellae were intensely stained (Fig. 4D). The uterine epithelium was only lightly stained (Fig. 4G).

#### Discussion

In the present study we could produce MoAbs specific to rFABP. These MoAbs could react with the native F. gigantica FABP at MW 14.5 kD represented as closely aligned double bands in immunoblots of whole-body (WB) and tegumental (TA) extracts, and the excretion-secretion material of the adult parasites. Smooker et

al. (1997) could also identify two isoforms of native *F. gigantica* FABP with similar MW. In contrast, it has been shown by many studies that *F. hepatica* has at least three isoforms of the cytoplasmic FABP family (Rodriguez-Perez et al., 1992; Chicz, 1994; Bozas and Spithill, 1996). Their molecular weight range between 14-16 kD with 127-133 amino acids in length (Hillyer, 1985; Hillyer et al., 1987; Veerkamp et al., 1991; Rodriguez-Perez et al., 1992). In comparison, homologous protein in *S. mansoni* has a MW about 12 kD (Hillyer et al., 1988a) and exhibited cross reactivity with *F. hepatica* FABP as well as cross protection for both species of parasites (Hillyer et al., 1988b). Analysis of cDNAs indicated that FABP in the two species showed 44% identity (Moser et al., 1991; Rodriguez-Perez et al., 1992). Our MoAb could detect only two isoforms of the *F. gigantica* FABP family which may possess similar epitopes. These two isoforms were also detected by polyclonal antibodies against native FABP. In comparison to the native FABP, rl'ABP that reacted with all MoAbs has a higher MW of 20 kD. The higher MW of rFABP is due to the addition of 31 amino acids for cloning and purification purposes as mentioned in Materials and methods.

The immunolocalization experiment demonstrated that FABP have a wide distribution in almost all tissues of the parasites. However, it has the highest concentration in one type of parenchymal cells which forms the major stroma or general packing tissue between epithelia lining the tegument, digestive, reproductive and urinary tracts; whereas two other types of parenchymal cells exhibit less staining intensity and thus probably contained a lower concentration of FABP. In contrast, the relative concentration of FABP in the caccal epithelium and tegument which were exposed to the hosts' fluid and thus thought to be involved in the initial uptake of fatty acids was quite low. It is possible that after the uptake through these two kinds of epithelia, fatty acids and cholesterol could be concentrated and stored in the first type

of parenchymal cells which acts as the intermediary in supplying these building block molecules to other kinds of cells that they maintain close contact. Some of the latter, such as, the tegument may require a significant quantity of lipids for the synthesis of the surface membrane which has a high rate of turn over for the parasite's homeostasis and protection (Hanna, 1980).

In addition to *F. gigantica* native FABP these MoAb also recognized similar sized antigens in *S. mansoni*, while no cross reactions were detected against antigens from other trematode parasites, including *Paramphistomun* spp. and *Eurytrema* spp. As has been reported, the strong cross reaction and cross protection between the FABP of *Fasciola* and *Schistosoma* are due to the high degree of conservation of 43% amino acid sequence identity (Smooker et al., 1997). In fact, FABP is considered to be one of the most promising vaccine candidates that could confer dual protection against fasciolosis and schistosomiasis (Casanueva et al., 2001). Vaccination against FABP may interfere with the processes of fatty acid and cholesterol uptakes and thus damage the structural integrity of many tissues, especially the surface membrane of the tegument, which have high need of these molecules for their building blocks. Furthermore, because of their specificities to only *Fasciola* and *Schistosoma* these MoAb may be good candidates for immunodiagnosis which will be further investigated.

#### Acknowledgements

This work was supported by the Thailand Research Fund (Senior Research Scholar Fellowship to Prasert Sobhon) and the National Center for Genetic Engineering and Biotechnology, NSTDA, (grant # BT-B-06-2B-14-004 to Vitoon Viyanant).

#### References

- Abane, J.L., Oleaga, A., Ramajo, V., Casanueva, P., Arellana, J.L., Hillyer, G.V., Muro, A., 2000. Vaccination of mice against Schistosoma bovis with a recombinant fatty acid binding protein from Fasciola hepatica. Vet. Parasitol. 91, 33-42.
- Bozas, S.E., Spithill, T.W., 1996. Identification of 3-hydroxyproline residues in several proteins of *Fasciola hepatica*. Exp. Parasitol. 82, 69-72.
- Casanueva, R., Hillyer, G.V., Ramajo, V., Oleaga, A., Espinoza, E.Y., Muro, A., 2001. Immunoprophylaxis against *Fasciola hapatica* in rabbits using a recombinant Fh 15 fatty acid-binding protein. J. Parasitol. 87, 697-700.
- Chicz, R.M. 1994. Submitted to the protein sequence database, August 1994. Accession No. A44638.
- Esteves, A., Joseph, L., Paulino, M., Ehrlich, R., 1997. Remarks on the phylogeny and structure of fatty acid binding proteins from parasitic platyhelminths. Int. J. Parasitol. 27, 1013-1023.
- Estuningsih, S.E., Smooker, P.M., Wiedosari, E., Widjajanti, S., Vaiano, S., Partoutomo, S., Splithill, T.W., 1997. Evaluation of antigens of *Fasciola gigantica* as vaccines against tropical fasciolosis in cattle. Int. J. Parasitol. 27, 1419-1428.
- Grams, R., Vichasri-Grams, S., Sobhon, P., Upatham, E.S., Viyanant, V., 2000.

  Molecular cloning and characterization of antigen encoding genes from *Fasciola gigantica*. In: Sirisinha, S., Chaiyaroj, S.C., Tapchaisri, P. (Eds.), International

- Proceedings of the 2<sup>nd</sup> Congress of the Federation of Immunological Societies of Asia-Oceania, Bangkok, Thailand, January 23-27. Monduzzi Editore, Bologna, Italy, pp. 39-43.
- Hanna, R.E., 1980. Fasciola hepatica: Glycocalyx replacement in the juvenile as a possible mechanism for protection against host immunity. Exp. Parasitol. 50, 103-114.
- Hillyer, G.V., 1985. Induction of immunity in mice to Fasciola hepatica with a Fasciola/Schistosoma cross reactive defined immunity antigen. Am. J. Trop. Med. Hyg. 34, 1127-1131.
- Hillyer, G.V., De Galanes, M.S., Garcia Rosa, M.I., Montealegre, F., 1988a. Acquired immunity in schistosomiasis with purified *Fasciola hepatica* cross reactive antigens. Vet. Parasitol. 29, 265-280.
- Hillyer, G.V., Garcia Rosa, M.I., Alicea, H., Hernandez, A., 1988b. Successful vaccination against murine Schistosoma mansoni infection with a purified 12 kD Fasciola hepatica cross reactive antigen. Am. J. Trop. Med. Hyg. 38, 103-110.
- Hillyer, G.V., Haroun, E.T., Hernandez, A., De Galanes, M.S., 1987. Acquired resistance to Fasciola hepatica in cattle using a purified adult worm antigen. Am. J. Trop. Med. Hyg. 37, 363-369.
- Lowry, O.H., Rosenbrough, N.J., Farr, S.L., Randal, R.J., 1951. Measurement of protein with the folin phenol reagent. J. Biol. Chem. 193, 265-275.
- Meyer, F., Myer, H., Bueding, E., 1970. Lipid metabolism in the parasitic and free-living Flatworms, *Schistosoma mansoni* and *Dugesia dorotocephala*. Biochim. Biophys. Acta 210, 257-266.

- Moser, D., Tendler, M., Griffiths, G., Klinkert, M.Q., 1991. A 14-kD Schistosoma mansoni polypeptide is homologous to a gene family of fatty acid binding proteins.
  J. Biol. Chem. 266, 8447-8454.
- Muro, A., Ramajo, V., Lopez, J., Simon F., Hillyer, G.V., 1997. Fasciola hepatica: vaccination of rabbits with native and recombinant antigens related to fatty acid binding proteins. Vet. Parasitol. 69, 219-229.
- Rodriguez-Perez, J., Rodriguez-Medina, J.R., Garcia-Blanco, M.A., Hillyer, G.V., 1992. Fasciola hepatica: molecular cloning, nucleotide sequence, and expression of a gene encoding a polypeptide homologous to a Schistosoma mansoni fatty acidbinding protein. Exp. Parasitol. 74, 400-407.
- Smooker, P.M., Hickford, D.E., Vaiano, S.A., Spithill, T.W., 1997. Isolation, cloning and expression of fatty-acid binding proteins from *Fasciola gigantica*. Exp. Parasitol. 85, 89-91.
- Veerkamp, J.H., Peeters, R.A., Maatman, R.G., 1991. Structural and functional features of different types of cytoplasmic fatty acid-binding proteins. Biochim. Biophys. Acta 1081, 1-24.
- Viyanant, V., Gajanadana, O., Upatham, E.S., Sobhon, P., Kruatrachue, M., Ahmed, S., Ardseungnoen, P., 1993. Monoclonal antibodies against Schistosoma mekongi surface tegumental antigens. Southeast Asian J. Trop. Med. Pub. Hith. 24, 484-488.

# Explanations of figures

- Fig. 1. A. Immunoblotting patterns of recombinant FABP reacted with myeloma culture fluid (CF-lane 1), normal mouse serum (NMS-lane 2), cow immunized serum (CIS-lane 3), monoclonal antibodies 3D4-12 (lane 4), 3D8-1 (lane 5), 3D8-6 (lane 6), 5C5-1 (lane 7), and 6F3-2 (lane 8). SD is the lane containing standard molecular weights.
- **B.** Immunoblotting patterns of *F. gigantica* whole body antigens (WB) reacted with myeloma culture fluid (CF-lane 1), normal mouse serum (NMS-lane 2), cow immune serum (CIS-lane 3), monoclonal antibodies 3D4-12 (lane 4), 3D8-1 (lane 5), 3D8-6 (lane 6), 5C5-1 (lane 7), and 6F3-2 (lane 8).
- Fig. 2. A. Immunoblotting patterns of *F. gigantica* whole body antigens (WB) reacted with myeloma culture fluid (CF-lane 1), normal mouse serum (NMS-lane 2), CIS (lane 3); and excretion secretion (ES-lane 4), tegumental (TA-lane 5) and whole body (WB-lane 6) antigens blotted with MoAb clone 6F3-2. Other clones of MoAb showed similar pattern and were not shown.
- B. Immunoblotting pattern of WB antigens with culture fluid (CF-lane 1), normal mouse serum (NMS-lane 2), cow immune serum (CIS-lane 3), and ES (lane 4), TA (lane 5), WB (lane 6) antigens with polyclonal antibodies against native FABP.
- Fig. 3. Immunoblotting patterns of WB antigens from F. gigantica (lane 4), S. mansoni (lane 5), E. pancreaticum (lane 6) and Paramphistomum spp. (lane 7) with MoAb 6F3-2. The controls show WB antigen reacted with myeloma culture fluid

(CF-lane 1) and normal mouse serum (NMS-lane 2) and cow immune serum (CIS-lane 3). Other clones of MoAb showed similar pattern and were not shown.

Fig. 4. Light micrographs of F. gigantica frozen sections stained by immunoperoxidase technique, using monoclonal antibodies as primary antibody and biotinylated rabbit antimouse IgG as secondary antibody. (Only sections stained with MoAb 6F3-2 were shown.)

A. A low magnification micrograph of the cross section of an adult parasite's body, showing intense staining in parenchymal cells (Pc) which form the general packing tissue between the tegument (Tg) and other organs (Testis-Te; Bladder-Bl; Caecum-Ca; Muscle-Mu).

**B.** A high magnification micrograph, showing intensely stained processes of parenchymal cells (arrow heads) running between muscle cells (Mu) towards the tegument (Tg), which is only lightly stained except at the surface membrane (arrows) and the basal cytoplasm which appears more intensely stained. Parenchymal cells showed variation in staining from the highest to the lowest intensities in Pc<sub>1</sub>, Pc<sub>2</sub> and Pc<sub>3</sub>.

C, D, E. Higher magnification micrographs of the interior of the adult parasites' bodies, showing in C intensely stained type I parenchymal cells (Pc<sub>1</sub>) and their processes (arrow heads), and less intensely-stained types 2, 3 parenchymal cells (Pc<sub>2</sub>, Pc<sub>3</sub>). Vitelline cells (Vg) are not stained. In D, most of the cytoplasm of caccal epithelium (Ep) is lightly stained, while the apical cytoplasm and lamellae (arrows) and content of the caecal lumen (Ca-arrow head) are intensely stained. In E and F, the testicular (Te) and ovarain (Ov) cells exhibit moderate staining, especially those lying

on the periphery of the gonadal follicles (arrow heads). In G, the uterine epithelium (Ut-Ep) is only lightly stained.

MW(kD	)	CI	FNMS	s cis	304-12	308-1	308-8	505-1	6F3-2	
66								7	1	
45								1		
31		4	. •	1						
21.5			:	- And Market	Revent	knavód	İveiq	house	-	
14.5								. !	1	
					rFΑ	ABP				
	SD	1	2	3	4	5	6	7	8	A

MM(kD) CE NWS CIS 20 4.12 30 8.1 50 5.1 50 5.1

66

45

31

21.5

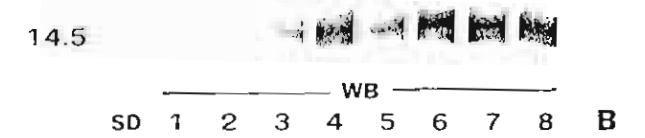
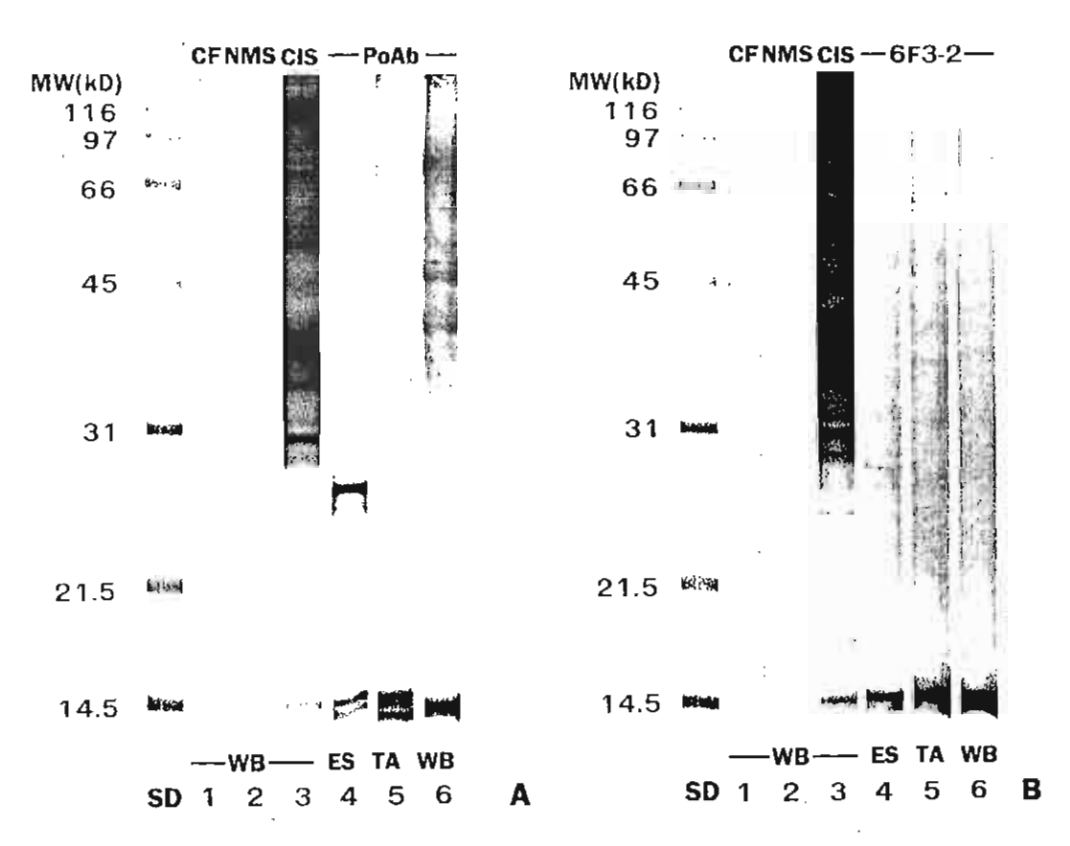
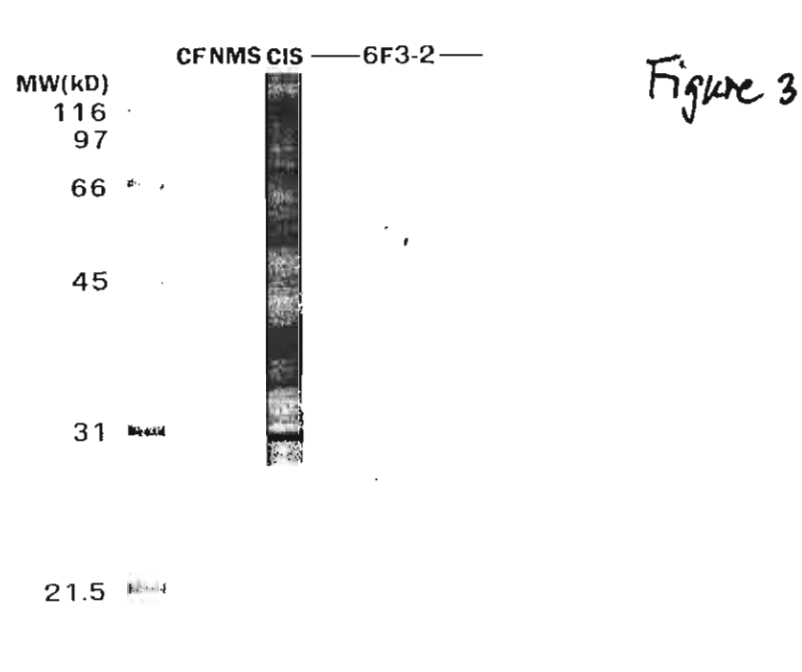
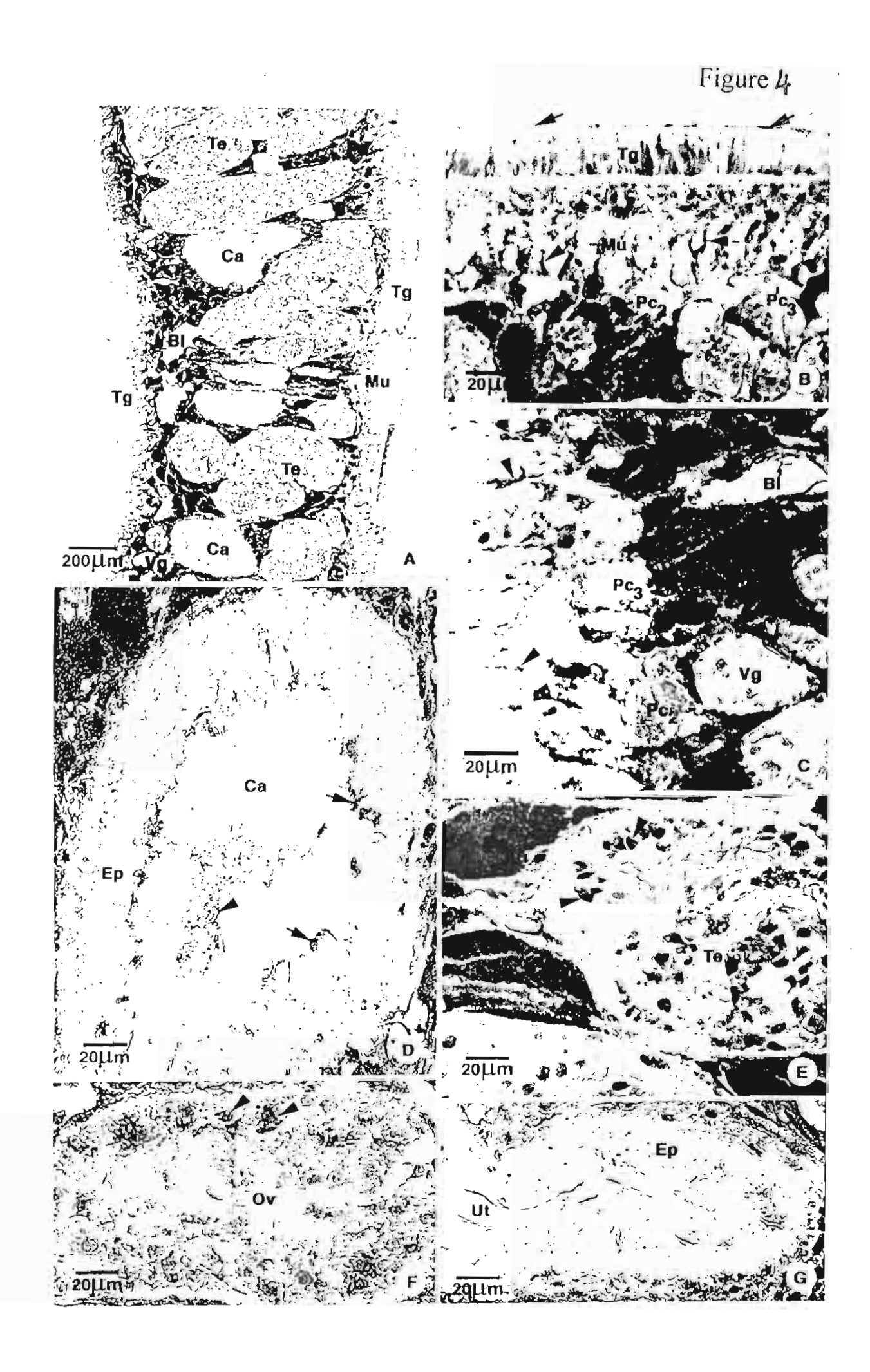


Figure 2





14.5

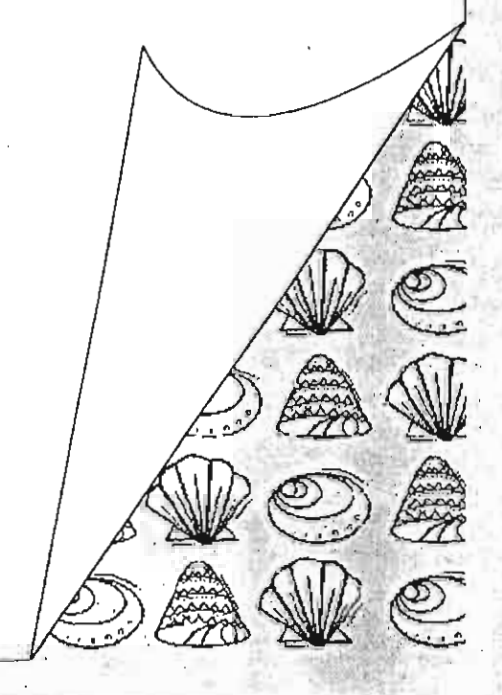


หนังสือ (International Proceedings)

# MOLLUSK RESEARCH IN ASIA

- PROCEEDINGS OF THE MEETING ON AQUACULTURE AND GENETICS OF TROPICAL OYSTER, ON MAY 1-2, 1997
- Proceedings of the Special Session on Mollusk Research in Asia held at the  $5^{\text{th}}$  Asian Fisheries forum, on November 12, 1998





# GAMETOGENESIS, REPRODUCTIVE CYCLE AND DEVELOPMENT OF GONADS IN Haliotis asinina LINNAEUS

PRASERT SOBHON<sup>1</sup>, SOMJAI APISAWETAKAN<sup>1</sup>, MALEE CHANPOO<sup>1</sup>, CHAITIP WANICHANON<sup>1</sup>, VICHAI LINTHONG<sup>1</sup>, AMPORN THONGKUKIATKUL<sup>3</sup>, PADERMSAK JARAYABIIAND<sup>4</sup>, MALEEYA KRUATRACIIUE<sup>2</sup>, SUCIIART UPATHAM<sup>3</sup>, AND TANATE POOMTHONG<sup>5</sup>

Departments of Anatomy<sup>1</sup> and Biology<sup>2</sup>, Faculty of Science, Mahidol University, Department of Biology<sup>3</sup>, Faculty of Science, Burapha University, Department of Marine Science<sup>4</sup>, Faculty of Science, Chulalongkom University, Bangkok, and Coastal Aquaculture Development Center<sup>6</sup>, Department of Fishery, Ministry of Agriculture and Cooperatives, Klong Wan, Prachuabkirikhun, Thailand.

ABSTRACT The gonad histology, ultrastructure and gametogenic processes of Haliotis asinina, a species of abalone found along the coast of Thailand, were studied by light and electron microscopies. The outer gonadal wall consists of fibro-muscular tissue forming a capsule with connective tissue septa or trabeculae that partition the gonad into compartments, where gonial and germ cells are attached to and surround each trabecula, thus forming oogenetic or spermatogenic unit. Within the connective tissue of trabeculae are vessels containing haemolymph surrounded by muscle cells, fibroblasts, and granulated endocrine-like cells. Germ cells in oogenetic units could be classified into six stages according to their histological and ultrastructural characteristics: oogonium and five stages of oocytes, i.e., Oc<sub>1</sub> with light to intense basophilia and abundant polyribosomes, with some in large aggregates; Oc<sub>2</sub> with intense basophilia, oil droplets, numerous well developed Golgi complexes and rough endoplasmic reticulum, but little secretory granules; Oc<sub>3</sub> with a few yolk granules and 2 types of cortical granules; Oc<sub>4</sub> with increasing number of yolk granules, numerous cortical granules and thin jelly coat; and Oc<sub>3</sub> is the mature ovum with 2 types of yolk granules, numerous cortical granules and fully formed jelly coat. The cells in spermatogenetic process could be classified according to the pattern of chromatin condensation into thirteen stages: spermatogonium, five stages of primary spermatocytes, secondary spermatocyte, four stages of spermatids and two stages of spermatids and two stages of spermatids.

The gonads of *H. asinina* reared in land-based culture system exhibit five phases of reproductive cycle during the year; these are proliferative, premature, mature, spawning and spent phases. Gonads in proliferative and premature phases contain primarily gonial cells, early occytes<sub>1-3</sub> and spermatocytes, while mature phase contains mainly late stage cells, i.e., occytes<sub>4-5</sub> in overy and spermatids and spermatozoa in testis. The spawning phase occurs at least twice during each year: from March to April and August to October in females, and with similar intervals but slightly prolonged duration in males. Spent phase, occurring after the period of spawning, is characterized by a complete discharge of gamete cells and the breakdown of connective tissue stroma. It takes approximately 5 to 6 months for gonads to regenerate their connective tissue stroma and germ cell population, and finally become repleted with mature cells again.

In developing II. asinina definitive gonads appear to be clearly separated from hepatopanereas at 4 months. Histologically, gonial cells appear at 5 months, early spermatocytes and oocytes (Oc<sub>1.2</sub>) at 6 to 7 months. While spermatids, spermatozou could arise in the gonads as early as 6 to 7 months, mature oocytes (Oc<sub>4.5</sub>) occur much later at 10 to 11 months. The mate animals tend to reach full sexual maturity and start normal reproductive cycle as early as 8 to 9 months, while female animals reach sexual maturity and start reproductive cycle around 11 to 12 months.

KEY WORDS: Haliotis asinina, gametogenesis, reproductive cycle, gonad development

#### INTRODUCTION

There are three species of abalone along the Thai coasts, namely, *H. asinina*, *H. ovina*, *H. varia* (1, 2, 3), which are also distributed generally over the Indo-western Pacific area, especially in coastal reef zones of Southeast Asia (4, 5). These abalone species are found along the Thai Gulf and Andaman Sea, usually in the crevices on coral and socky reefs, at the depth of 1 to 7 m of water (1, 2, 3, 6). Among the three species, *H. asinina* has the largest size and the most economic potential because of their maximum proportion of flesh (7) and good taste. *H. asinina* is primarily found off

the eastern coast of the Gulf of Thailand around Chon Buri, Rayong and Trad provinces (6, 8). Since collection from natural habitat could not keep pace with market demand, an efficient aquaculture system for this abalone is required. However, there are still lack of certain aspects of knowledge that could aid the large scale production of larvae for aquaculture. These are: 1) the prohable spawning periods and the frequencies of spawning of land-cultured broodstocks during the year; 2) the age when the abalone reach full sexual maturity and can be used as broodstocks; and 3) the possibility of using artificial means to induce spawning when the gonads are fully developed, so that mature gamete

<sup>\*</sup> This investigation was supported by the Thailand Research Fund (Contract BRG4080004 and Senior Research Scholar Fellowship to Prasert Sobhon).

cells from both sexes could be obtained simultaneously.

Among abalone species found in Thailand, preliminary study in H. varia around Bon Island, Pluket, showed that spawning occurred at several intervals throughout the year during January-February, April-May, June-July and November-December (9). Gametogenic cycle was also studied in another species, H. ovina, at Khangkao Island, Chon Buri province (10), in which the spawning period occurred between June and November. So far there has not yet been any studies of the gametogenic cycle as well as the development and structure of reproductive organs in 11. asinina. Therefore, the aims of the present study are to investigate the reproduction of H. asinina that have been reared in land-based culture system with respect to 1) the gonadal histology and the gametogenic processes, especially the classification of various stages of germ cells in the testis and ovary of this abalone based on light and electron microscopic observations; 2) possible cyclical pattern of gonadal histology during different months of the year; and 3) the development of the gonads and the ages that abalone of both sexes reach full sexual maturity. The knowledge gained could be applied in determining the appropriate time for induction of spawning, and to increase gamete production, for the improvement of aquaculture system of this abalone species.

#### MATERIALS AND METHODS

#### Collection of abalone specimens

Abalone from land-based culture system are provided by the Coastal Aquaculture Development Center, Prachaubkirikhun province, and Marine Biological Station, Chulalongkorn University, Angsila, Chon Buri province. They are kept in concrete tanks housed in the shade, which are well flushed with mechanically circulated filtered sea water and air delivery system to maintain the controlled environment. The optimum level of salinity is about 22.5-32.5 ppt and the temperature is about 22-26°C (7). They are fed with a diet of macroalgae (usually *Graciluria* spp. and *Laminaria* spp.), supplemented with artificial food for abalone.

For studies of the gonadal histology, ultrastructure and the cyclical changes during the year, adult abalone, aged at least 24 months, were collected monthly for a period of one year. The fixed gonads were prepared for light and electron microscopic observations by the paraffin, semithin, and conventional TEM methods.

For development of the gonads, samples of juvenile abalone reared in the closed-culture system

as mentioned above were collected monthly from the age of 3 to 12 months, and the gonads were processed for light microscopic observations.

#### Light Microscopy

Abalone were anesthetized in magnesium chloride (MgCl2) for one hour, for paraffin sections the gonads were cut and fixed in either Bouin's solution, or 3% glutaraldehyde in 0.1M sodium cacodylate buffer pH 7.4, at 4°C, for overnight. The tissue blocks were then washed in 70% ethyl alcohol for removal of the Bouin's fixative, and glutaraldehyde fixative was removed by washing with phosphate buffer three times. Then, the specimens were dehydrated in graded series of ethyl alcohol (70-100%) for 30 minutes each, cleared with dioxane, infiltrated and embedded in paraffin wax. Blocks of specimens were sectioned at 5-micron thick, and finally stained with heamatoxylin-eosin, or PASheamatoxylin, and observed in an Olympus Vanox light microscope.

#### Transmission Electron Microscopy

For semithin sections and TEM studies, gonads were cut into very small pieces and fixed in a solution of 3% glutaraldehyde in 0.1M sodium cacodylate buffer pH 7.4, at 4°C, for overnight. The specimens were post-fixed in 1% osmium tetroxide in 0.1M sodium cacodylate buffer, at 4°C, for 2 hours. Then, they were dehydrated in graded series of ethanol (50-100%) for 30 minutes each, cleared in two changes of propylene oxide, infiltrated in a mixture of propylene oxide and Araldite 502 resin at the ratios of 3:1 for 1 hour, 2:1 for 2 hours and 1:2 for overnight, then embedded in pure Araldite 502 resin for at least 6 hours, and finally polymerized at 30°C, 45°C and 60°C for 24, 48 and 48 hours, respectively. Blocks of specimens were sectioned at 1-micron thickness by ultramicrotome and stained with Methylene blue for light microscopic observations, and ultrathin sections were cut and stained with lead citrateuranyl acetate and viewed under a Hitachi TEM H-300 at 75 kV.

1

c

0

ď

fi

aj

SJ

be

as

cf

m

ge

51;

Sp

10

Wi

пк

ble

#### RESULTS

#### 1. Gonadal Histology

The conical organ consists of the hepatopancreas surrounded by the testis or ovary (Fig.1C,D). At the base of the organ, the hepatopancreas appears large and occupies most of the cross-sectional profile (Fig.1C); while it becomes smaller towards the tapered end of the organ where most of the tissue belongs to the gonads (Fig.1D). Both testis and ovary are surrounded by a capsule which is composed of the outer single layer of epithelial cells, and the inner

layer of dense collagenous fibers mixed with smooth muscle cells (Fig.1K, 2D). The thickness of this capsule varies according to the gonadal cycle during the year.

The connective tissue from the capsule extends perpendicularly into the interior of the gonad to form septa or trabeculae that are branched, and connected at the innermost ends with the thin loose capsule of hepatopancreas. As a result the gonads are partitioned into small compartments, each containing various stages of maturing germ cells (Fig. 1E, 1J). Within the connective tissue of each trabecula, there are small vessels running through its whole course (Fig.1F, 1L,M), which may be capillaries that branch out from the larger Around the capillaries, subcapsular vessels. parallel to the long axis of the trabeculae, there are packs of smooth muscle cells and collagen fibers that are intermingled with small cells exhibiting dense ellipsoid nuclei (Fig.1K, 1M). Some of the latter may be fibroblasts, while others may be follicular or supporting cells that surround oogonia and developing oocytes. Some small cells contain granules that show similar characteristics as endocrine cells.

Each trabecula acts as the axis on which growing germ cells are attached (Fig.1E,F, 1J,M). Early stage cells, such as spermatogonia, initial stages of primary spermatocytes and oogonia, are closely adhered to the trabeculae. Middle stage germ cells, such as secondary spermatocytes and developing oocytes, are more detached and appear further away from the trabeculae; while late stage cells, such as spermatids, spermatozoa and mature oocytes, are completely detached and move to the outermost region from the axis. Such an appearance gives rise to a discrete group of germ cells surrounding each trabecula, which is termed spermatogenic or oogenic unit.

#### 2. Classification of Germ Cells

Germ cells appearing in the gonads could be classified, according to their structural features as observed under the light and transmission electron microscopes, as follows:

2.1 Spermatogenic cells Based on the nuclear characteristics and the cell sizes, the male germ cells of *II. asinina* can be classified into 13 stages.

Spermatogonium (Sg) (Fig.1G) Sg is a spherical or oval-shaped cell with diameter about 8-10 μm. Its nucleus is round or slightly indented with diameter about 6-7 μm. The nucleus contains mostly euchromatin with only small chromatin blocks attached to the inner surface of nucleur

envelope. The nucleolus is prominent and stands out from the rather transparent nucleoplasm. Sg are bounded to traheculae.

Primary spermatocytes (PrSc) (Fig.1G-H, 4A-C) PrSc consists of 5 stages, i.e., leptotene (LSc), zygotene (ZSc), pachytene (PSc), diplotene (DSc), and diakinetic or metaphase (MSc) stages. The early cells (from LSc to PSc) are round and become increasingly larger, then they (from DSc to MSc) are gradually decreased in size. Another distinctive differences among various stages of PrSc is the pattern of chromatin condensation and the relative amount of euchromatin versus heterochromatin.

Leptotene spermatocyte(LSc) (Fig.1G,H, 4A) These round-shaped cells are larger than Sg with diameter about 10-12  $\mu m$  and also contain large round nuclei, each with diameter about 8  $\mu m$ . There is a thin rim of heterochromatin along the nuclear envelope and small blocks of heterochromatin scattered evenly throughout the nucleus. The nucleolus is still present but not as prominent as in Sg.

Zygotene spermatocyte (ZSe) (Fig.1G,1I, 4A) ZSc has approximately the same size as LSc. The distinguishing features of ZSc is the heterochromatin blocks which are increasing in size and density, and they are coupled at many points by synaptonemal complexes. The nucleolus disappears completely.

Pachytene spermatocyte (PSe) PSc still shows round shape with slightly smaller size than those of LSc (about 8 μm in size and 5 μm in nuclear diameter). Under LM (Fig.1G,H) it is characterized by the heterochromatin which appears as long threads or thick fibers that are entwined into "bouquet pattern", and becoming visible throughout the nucleus. Under TEM (Fig.4A-C) these chromatin "threads" are actually thick blocks consisting of tightly packed 30 nm fundamental chromatin fibers.

Diplotene spermatocyte(DSe) (Fig.1G,H, 4A-C) T his cell resembles PSc, except the nucleus becomes smaller (about 4  $\mu m$ ), and the chromatin blocks become increasingly thicker and packed closer together in the denser nucleoplasm than in earlier stages.

Dinkinetic and Metaphase spermatocytes (MSe) (Fig.111, 4B,C) These stages exhibit thick chromosomes that move to the equatorial region, while the nuclear membrane disintegrates and completely disappears in MSc.

Secondary spermatocyte (SSc) (Fig.4B,C) SSc is a small round cell about 7 µm in diameter with the nucleus about 4 µm. They show thick chromatin blocks that are crisscrossing one another, thus appearing as checker-board or XY figures. The individual chromatin fibers in the block are loosened up, and each still maintains the size of 30 nm.

Spermatids (St) (Fig.1F-H, 4B,C) There are 4 stages of spermatids, i.e., spermatid I (St<sub>1</sub>), spermatid III (St<sub>3</sub>) and spermatid IV (St<sub>4</sub>) depending on the size, chromatin granulation and condensation. All stages are round or oval, and ranging in size from 6  $\mu$ m in St<sub>1</sub> to 3  $\mu$ m in St<sub>4</sub>.

Spermatid I (St<sub>1</sub>) (Fig.1G) St<sub>1</sub> can be distinguished by their chromatin which appears as fine granules under LM, that are uniformly spread throughout the nucleus. As a result the whole nuclei appear moderately dense without any intervening transparent areas of nucleoplasm. Under TEM the 30 nm chromatin fibers becomes loosely packed and uniformly distributed throughout the nucleus.

Spermatid II ( $St_2$ ) (Fig.1G,H) The general features of  $St_2$  are similar to those of  $St_1$  but the nucleus, which remains round, decreases in size and is located eccentrically within the cell. As a result the chromatin fibers become more closely packed, and the nucleus appears denser but still uniform.

Spermatid III (St<sub>3</sub>) (Fig.1G,H, 4B,C) The cell becomes smaller and assumes more oval shape with eccentrically-located and clongated nucleus. The chromatin begins to condense into dark blocks with intervening light area of nucleoplasm, individual chromatin fiber is enlarged to 40 nm.

Spermatid IV (St<sub>4</sub>) (Fig. III) The cell becomes smallest but still appears oval. Its chromatin becomes completely condensed, thus the nucleus appears rather opaque; however, the outlines of individual chromatin fibers could still be observed, and each is enlarged to 60 mm.

Spermatozoa (Sz) (Fig. IF-I, 4D) There are 2 stages of spermatozoa: Sz<sub>1</sub> is the immature spermatozoon that begins to show highly clongated nucleus with completely dense chromatin, thus the outlines of chromatin granules are barely discernible. There is a cap-like structure apposing on one side of the ellipsoid nucleus, which is the maturing acrosome. The tail is short with a pair of

centrioles moving to the neck region, from which the axonemal microtubules start to form.

In mature spermatozoa (Sz<sub>2</sub>) (Fig.1I, 4D) the nucleus is fully elongated and slightly tapered at the anterior end, with the size about 1x3 µm. The chromatin is completely dense and the anterior portion of the head is covered by acrosome with central core element (Fig.4D). Five globular mitochondria surround the centrioles in the neck region. Zig-zag microtubules link mitochondria to the plasma membrane covering the distal half of the nucleus. The tail is lengthened, and consists of 9+2 axonemal microtubule doublets surrounded by plasma membrane. Both immature and mature sperm are completely detached from the germinal epithelium and come to lie in the space between adjacent spermatogenic units (Fig. 11, 4B,D).

2.2 Oogenetic cells There are 6 stages of female germ cells of *H. asinina*, including oogonium and five stages of growing oocytes.

Oogonium (Og) (Fig.1K,L) Og is a round or oval-shaped cell, whose size is about 10-12 µm. Its nucleus is round and about 7 µm in diameter. It contains small blocks of heterochromatin attached to the inner surface of nuclear envelope, with the remaining majority appearing as euchromatin. The nucleolus is present but may not be as prominent as The cytoplasm is stained light blue by in Sg. heamatoxylin-cosin and methylene blue, which implies its basophilic property due to the presence of moderate amount of ribosomes. Og are attached to the capsular side of trabeculae and usually are concentrated in groups (Fig.1K,L). Each Og is surrounded by flat, squamous-shaped follicular cells.

Stage I Oocyte (Oc,) (Fig.1K,L, 5A-C) Oc, is a round or scallop-shaped cell that is closely adhered to the trabecula. It is about 15-24 jun in size, with a round nucleus about 12 µm in diameter. The nucleus exhibits densely packed chromatin in the form of numerous lampbrush chromosomes. The nucleolus is present but tends to be obscured by the rather dense chromatin and nucleoplasm. The cytoplasm is stained deep blue with heamatoxylin-eosin and methylene blue, which indicates its intense basophilic property, reflecting the presence of numerous polysomes, newly developed rough endoplasmic reticulum (RER) and Golgi complexes (Gc) as observed in TEM (Fig.5C). Newly released ribosomes are packed into large mass around nuclear envelope (Fig.5B). There is very few secretory granules. Due to its enlarged size each Oc, is surrounded by few follicular cells.

Stage II Oocyte (Oc2) (Fig.1K, L, 5D, 6A Oc2 becomes larger and transforms into columnar shape, with the cell size around 30x55 µm, and nuclear size about 22 um. It is still attached to the connective tissue of trabecula by the narrow part. and each Oc, is surrounded by several follicular The nucleus exhibits increasingly decondensed chromatin and nucleolus. Thus the nucleolus and nuclear membrane are clearly distinct due to the more transparent nucleoplasm and the presence of mostly euchromatin. The cytoplasm is stained light blue similar to Og, and contains cluster of clear lipid droplets (Fig.5D). At TEM level it was observed to contain numerous well-developed Gc, RER and still abundant ribosomes. There are 2 types of secretory granules: SG1 and SG2 (~330 and 450 nm in diameter) with electron lucent and electron dense matrix, respectively (Fig.6A,B).

Stage III Oocyte (Oc3) (Fig.1M, 6B) This cell becomes increasingly larger and assumes flask or pear shape, with the narrow side or base still attached to the connective tissue of trabecula. The cell size is about 35-70 µm, with the nuclear size about 20 um. The nucleus contains mostly most of the lampbrush euchromatin, as almost completely chromosomes become unraveled, and the nucleoplasm is quite transparent. The nucleolus is distinct and becomes enlarged due to the uncoiling of nucleolar chromatin. In addition to increasing number of clear lipid droplets, the cytoplasm begins to show reddish yolk platelets (Fig.1M) which are electron dense under TEM. Fine blue granules representing SG1 and SG2 are evenly distributed between lipid droplets and yolk At TEM these granules are seen concentrated around Gc (Fig.6B). Follicular cells surround both the cell body and its base near trabecula.

Stage IV Oocyte (Oc4) (Fig.2A,C, 6C) This cell is large and assumes a pear or polygonal shape, but still attached to trabecula by slender cytoplasmic process. The cell size is about 60-80  $\mu$ m, with nuclear size about 35 µm. The nucleus contains mostly euchromatin and completely transparent nucleoplasm (Fig.2A,C, 6C). Hence the nucleolus is clearly visible, and it also becomes enlarged due to the complete uncoiling of its chromatin. The cytoplasm is filled with reddish and electron dense yolk platelets (each about 1500-2500 nm in diameter) mixed with numerous lipid droplets (each about 1500-3000 nm in diameter) Fine blue-stained granules which (Fig. 6C). represent SG1 and SG2 are decreased in central area of the cytoplasm, since most are probably translocated to the area underneath the plasma membrane. A thin layer of jelly coat begins to form on the outer surface of the cell membrane (Fig.2C). This coat is PAS positive and may be formed by the released content of SG<sub>1</sub>, which were seen exocytosed at the oocyte's plasma membrane (Fig.6D). The coat is in turn surrounded by follicular cells.

Stage V Oocyte (Ocs) (Fig.2B-D) This is the fully mature oocyte before being released from the adult female. Ocs is the largest cells with polygonal or round shape, with the cell size about 80-140 µm and the nuclear size about 40 µm. The nucleus exhibits similar characteristics as that of Oc4, but with completely enlarged and clear nucleolus. Oc, could be divided into 2 subgroups based on the characteristics of volk platelets observed under LM (Fig.2D). The first subgroup contains small and similar size yolk platelets that are scattered evenly throughout the cytoplasm. In the second subgroup, the yolk platelets are variable in size, and most are large bodies that could be formed by the coalescence of the smaller yolk platelets. Stripe of fine blue granules are also located underneath the cell membrane as in Oc4 (Fig.2C,D). The thick PAS positive jelly coat attains its maximum thickness and is uniform around the outer surface of the cell membrane, but without the surrounding layer of follicular cells. Under TEM jelly coat appears fibrous in comparison to the amorphous appearance in Oc4 (Fig.6D). All Oc, are completely detached from the connective tissue of trabeculae.

#### 3. Reproductive Cycle

The reproductive cycle of *H. asinina* was assessed by observing the changes in the gonad histology, especially the characteristics of cellular association during one year period. The stages of gonad maturation during one reproductive cycle of the abalone cultured in a closed land-based system could be classified into 5 distinct phases as follows.

Proliferative phase (Fig.2E-I) This is a period in which gamete cells begin to regenerate to commence a new reproductive cycle. initiation of this phase, the gonads contain mainly early stage cells, and all of them are closely attached to the trabeculae. The ovary (Fig.2E,F) contains primarily Og, which usually form clusters near the capsular side, and Oc, and Oc, which are rapidly increased in number. In the testis (Fig.2G-1) there are mostly Sg and PrSc, but neither St nor Sz are present. The clusters of these early stage cells are located around the short and dilated trabeculae. The hepatopancreas is quite large in size and occupies most of the cross sectional profile of the conical organ when compared to the total gonad area. This phase usually occurs immediately after the spawning, and lasts for 2 months around April to May and October to November.

Premature phase (Fig.2J-M) This phase is the period when gametogenesis proceeds at full speed with rapid increase in numbers and sizes of various cells, while hepatopaucreas is slowly reduced in its relative size; the gonads become enlarged in volume and trabeculae become thinner. At the beginning, the ovary (Fig.2J,K) contains Og, Oc1, Oc2 and predominantly Oc3, most of which are still attached to the trabeculae; and later Oc4 and Ocs cells occur. The testis (Fig.21, M) contains mainly Sg, PrSc, increasing number of St and a few of Sz, all of which aggregate around the trabeculae. This phase lasts about 2 months following the proliferative phase, usually around May to June and January to February in female; and it takes place around April to May and December to January in male.

Mature phase (Fig.3A-E) This phase is a period of rapid growth of gonads which are reflected by striking differences in color between the two sexes. The rates of cells proliferation start to diminish, and the gonads contain primarily late stage germ cells, while only a few of the early stage cells are still present and restricted to area immediately around trabeculae. Hepatopancreas is further decreased in size, and trabeculae become In the ovary (Fig.3A,B) there are abundant Oc5, but only few remaining and widely scattered Oc1. All of Oc3 appear fully mature and are liberated into the lumen of oogenetic compartment. In the testis (Fig.3C-E) there are mostly late stage male germ cells, i.e., St and Sz. The most noticeable characteristics of the testis in this phase is the vast number of Sz, which lie in rows that in turn surround the earlier cell stages which are still closely attached to the trabeculae (Fig.3D). As a result the testis appears to have maximum density of late stage cells. Prior to spawning, all of Sz<sub>2</sub> are dispersed into gonadal himen and intermingled with other late stage cells (Fig. 3E). Thin bands of Sg and PrSc surrounding the trabeculae are still evident. This phase lasts for 2 months usually from June to July and February to March in both sexes.

Spawning phase (Fig.3F-J) This is the period when abalone are ready for breeding, during which the completely mature and viable eggs or sperm are released from the gonads. The gonads are significantly decreased in size, and the gonadal wall becomes wrinkle when compared with the former phase (Fig.3H). Mostly ripen sperm or eggs are discharged while the earlier stages of gamete cells are still attached to the dilated trabeculae. After spawning, the yellowish granular substances

(Fig.3G) remain in the lumen of gonadal compartments in both sexes. Spawning phase occurs at least twice during the one year period of observation, usually from August to October and March to April in female, and around August to October and February to March in male. In addition, partial spawning could be observed throughout the year in some males.

Spent phase (Fig.3K-N) This is the period after spawning when fully mature gamete cells are completely discharged. The gonads exhibit the breaking down of connective tissue stroma, and gametogenic activity momentarily cease. However, there are still clusters of gonial cells remain attached to parts of the gonads' capsule. As a result the gonads are greatly decreased in size and become creamy in color in both sexes. This quiescence gonads show small cross-sectional profiles in contrast to those of the hepatopancreas, which becomes very large in relative size (Fig.3M). This phase occurs after spawning around September to October and April to June in both sexes.

#### 4. Development of Gonads

In developing II. asinina, definitive gonads appear during 4 months. The initial sign is the separation of hepatopancreatic capsule into 2 separate layers. Clusters of gonial cells start to appear in the space between the two capsules. Definitive gonial cells, early oocytes and spermatocytes could be detected at 5 months, when the ovary could be distinguished from the testis by the presence of Oc, in contrast to primary spermatocytes. Oocytes and spermatocytes are increasing in number during 6 to 7 months. While testis are rapidly enlarging and surrounding almost half of the circumference of the conical organ, ovary is much less developed. Spermatids and spermatozoa are already present in large number as early as 6 to 7 month. By 8 to 9 month the testis becomes enlarged to almost completely surround the hepatopancreas, and it already contains fully mature male germ cells; while the ovary tends to be delayed in development and contains only early oocytes (Oc<sub>4-3</sub>). By 10 to 11 month the testis appears fully developed, while the ovary starts to enlarge substantially and mature oocytes (Oc4.5) begin to appear. Thus the male animals tend to reach full sexual maturity and start normal reproductive cycle as early as 8 to 9 months, while female animals reach sexual maturity and start reproductive cycle around 11 to 12 months.

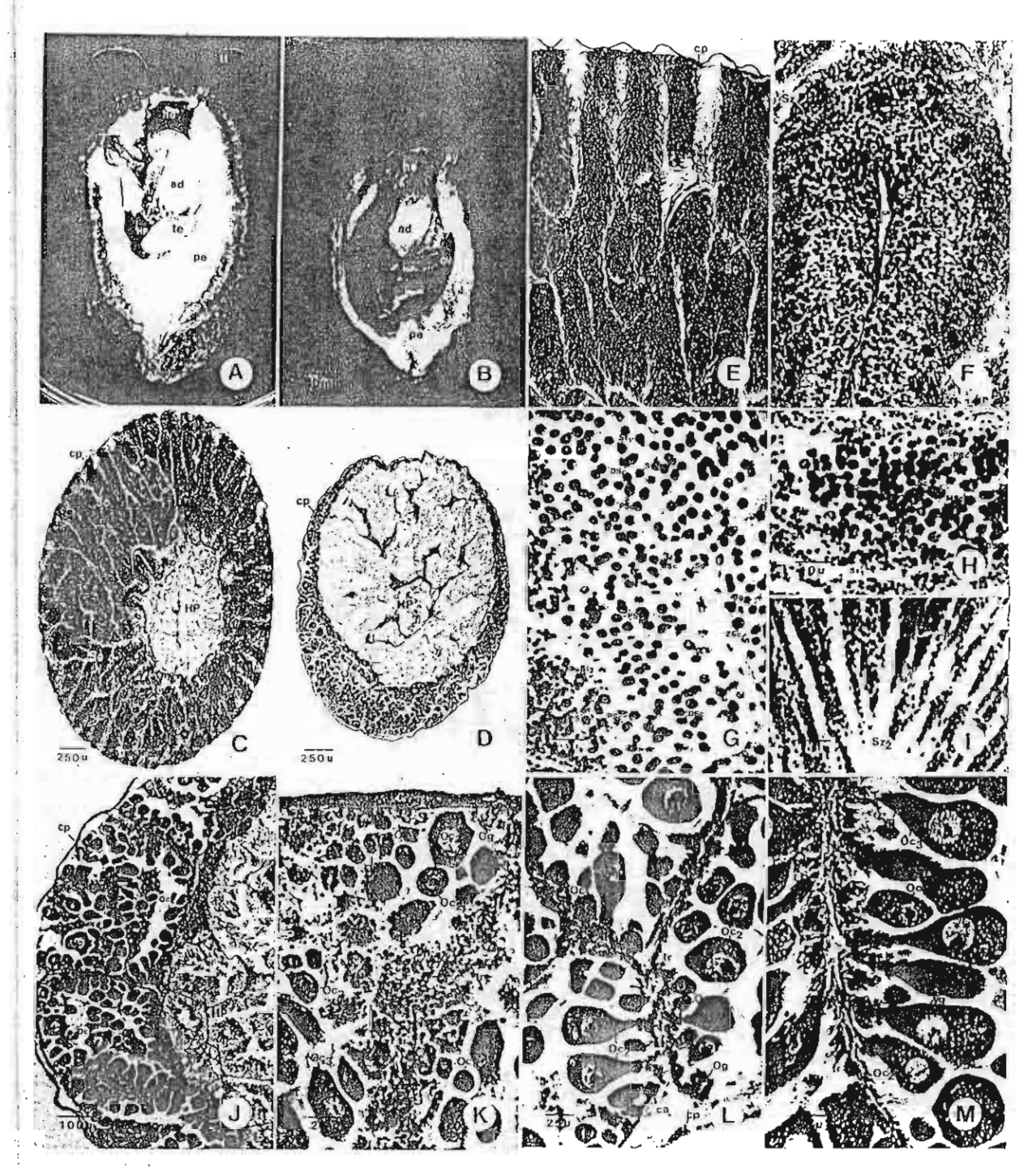


Fig.1 A,B) Dorsal views of shell-freed male abalone (A) and female (B) abalone in B, showing testis (te), ovary (ov), hepatopanereas (HP), adductor muscle (ad), pedal muscle (pe), head (he), eyes (ey), and tentacle (tt).

C) A cross-section of the testis, showing hepatopanereas (HP) surrounded by testicular tissue which is, in turn, surrounded by a thin connective tissue capsule (cp).

D) A cross-section of the overy, showing hepatopanerens (HP) surrounded by overian tissue and fibrous capsule.

E,F) A spermatogenic unit consists of a central trabeculae (tr) arising from capsule (cp), surrounded by various stages of germ cells. In F, a capillary (ca) is present inside each trabeculae, and successive maturing stages of germ cells lie at different distance from the connective trabecula (Se-spermatocyte, St-spermatid and Sz-spermatozoa).

G-I) Sections showing various stages of nucle germ cells surrounding each trabecula; they are spermatogonin (Sg), primary spermatocytes (USe-leptotene; ZSe-zygotene; PSe-pachytene; DSe-diplotene; MSe metaphase stage), spermatid (St<sub>1-2</sub>), and spermatozoa (Sz<sub>1-2</sub>). In I there are rows of fully mature spermatozoa (Sz<sub>2</sub>), which are the most typical characteristic in mature phase of male abalone.

there are rows of fully mature spermatozoa (Sz<sub>2</sub>), which are the most typical characteristic in mature phase of male abalone.

J) An opposite unit also consists of an axis of trabecula (tr) with closely attached early stage occytes (Oc<sub>1-3</sub>). The fully mature occytes (Oc<sub>3</sub>) are released into the central area of the compartment partitioned off by adjacent trabeculae.

K-M) Sections showing stage I, II and III oocytes (Oc<sub>1-3</sub>) which exhibit intensely basophilic cytophasm. In M there are stage III oocytes (Oc<sub>3</sub>) showing the presence of cosmophilic yolk granules (arrows) in the cytoplasm when compared with the former stage oocytes.

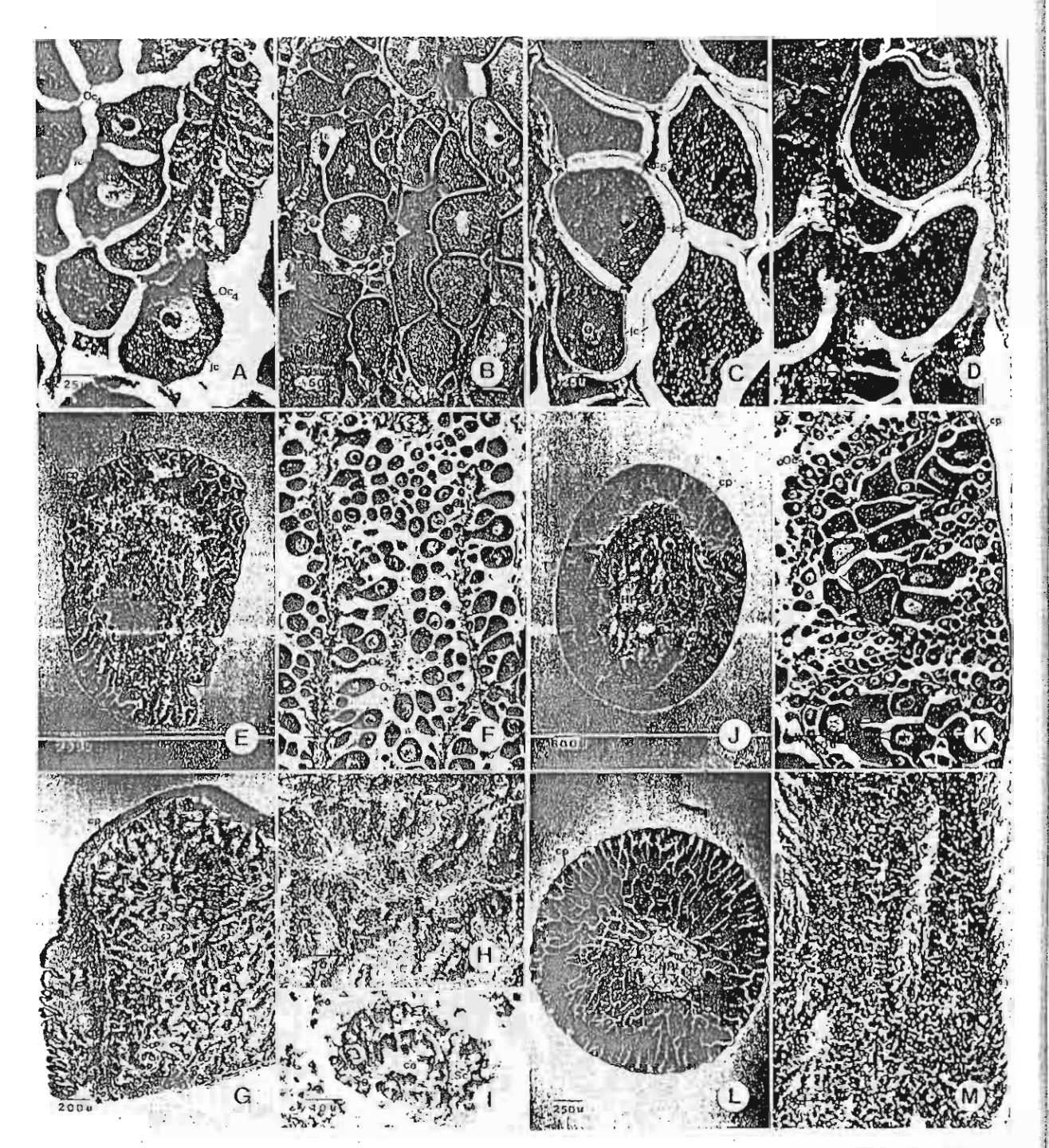
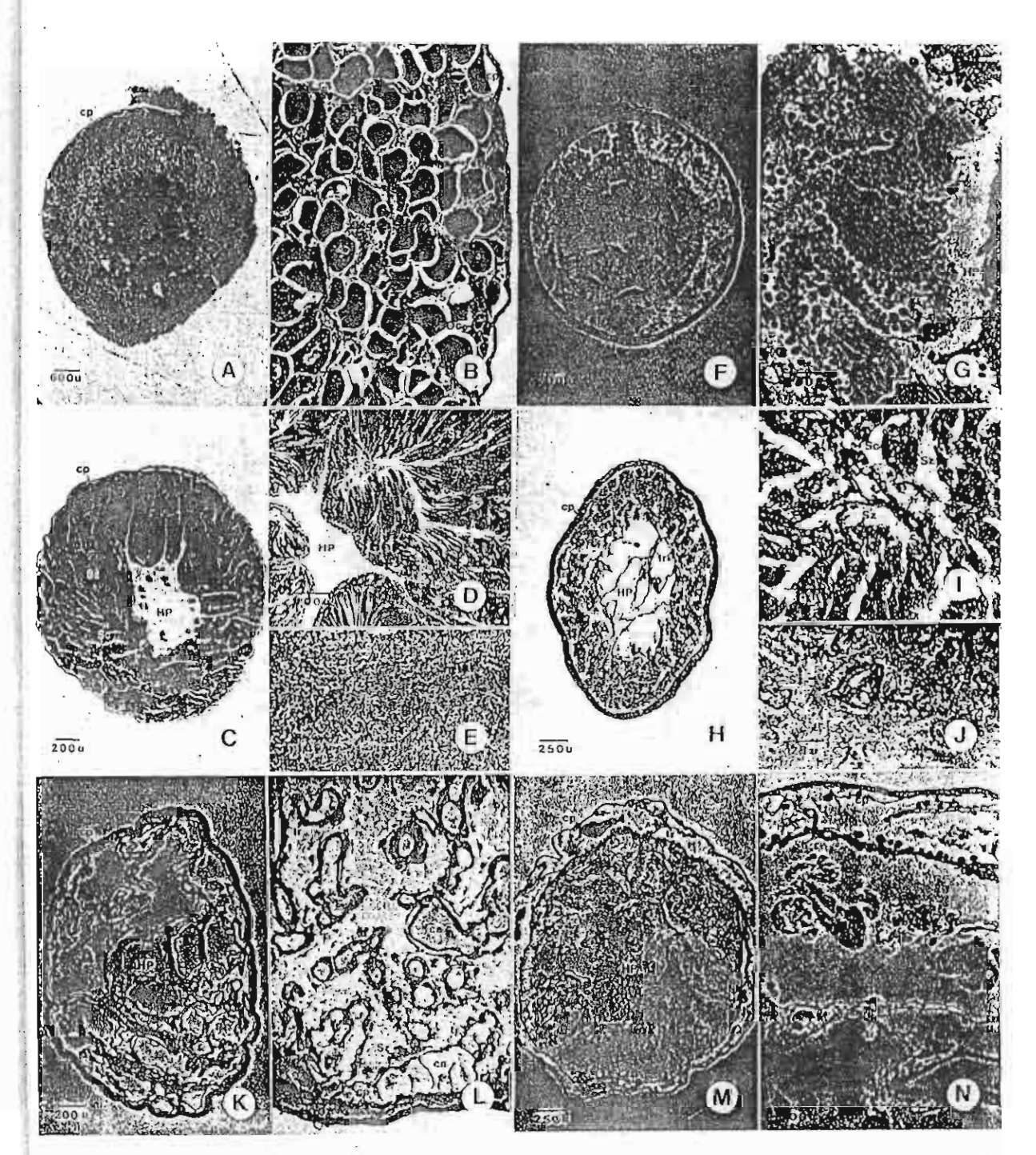


Fig.2 A-D) Sections showing stage IV and V (Oct.5), notice the first appearance of a thin jelly coat (je), which is PAS positive, and increasing number of cosmophilic yolk granules (yg) in Oct.5. The increasing amount of cuchromatin, which is pale stained, and the enlargement and vesiculation of nucleolus are also noticeable. Blue stripe underneath the cocyte's plasma membrane (arrow) is present in Oct.5. In D there are two subtypes of stage V cells: the upper cell (1) shows small and evenly distributed cosmophilic yolk granules, and the lower cell (2) shows large platelet of yolks.

E-I) Sections of "proliferative phase", showing the regeneration of gamete cells after spawning and spent phases. The ovary (E,F) contains only Oc<sub>1-2</sub>, which are rapidly increased in numbers. The testis (G-I) contains mostly Sg and LSc. Trabeculae, which are depleted of cells and breaking down in spent phase, start to regenerate and appear short and dilated.

Fig.3

J-M) Sections of "premature phase", showing rapid merease in numbers and sizes of various cells. The overy (J,K) contains mostly early stage exceptes (Oc<sub>1-1</sub>) and late stage eocytes (Oc<sub>4-5</sub>) start to appear and gradually increase in numbers. The testis (L,M) contains various stage of primary spermatocytes (PrSe), spermatid (St) together and a few spermatozoa (Sz); all of which are located close to the trabeculae.



関係はではおりのにはいいろう

BENEFIT TO STATE OF S

ここであり、 「かってもす

S d

П

Fig.J.A.E.) Sections of "mature phase", showing rapid growth of the gonads. The ovary (A,B) contains primarily fully mature Ocs with only a few widely scattered early stage cells (Ocs...). The testis (C-E) contains mostly late spermatids (St) and spermatozon (Sz), which lie in rown and at low power appear streaky (D). Finally they become dispersed and released into luminal area of the testis.

F-J) Sections of "spawning plants", showing the period when abalone release the viable sperm or eggs from the gonads. The ovary (F,G) contains only the earlier stage occytes which are still attached to the dilated trabeculae. Some yellowish granular substances (arrow) is present in the ovarian lumen. The testis (H-J) contains only early stage of male germ cells with a few of spermatozon (Sz).

K-N) Sections of "spent phase", showing the complete discharge of gamete cells, and the breaking down of trabeculae and associated connective tissues in both sexes. Notice the hepatopaneress which becomes larger in relative size.

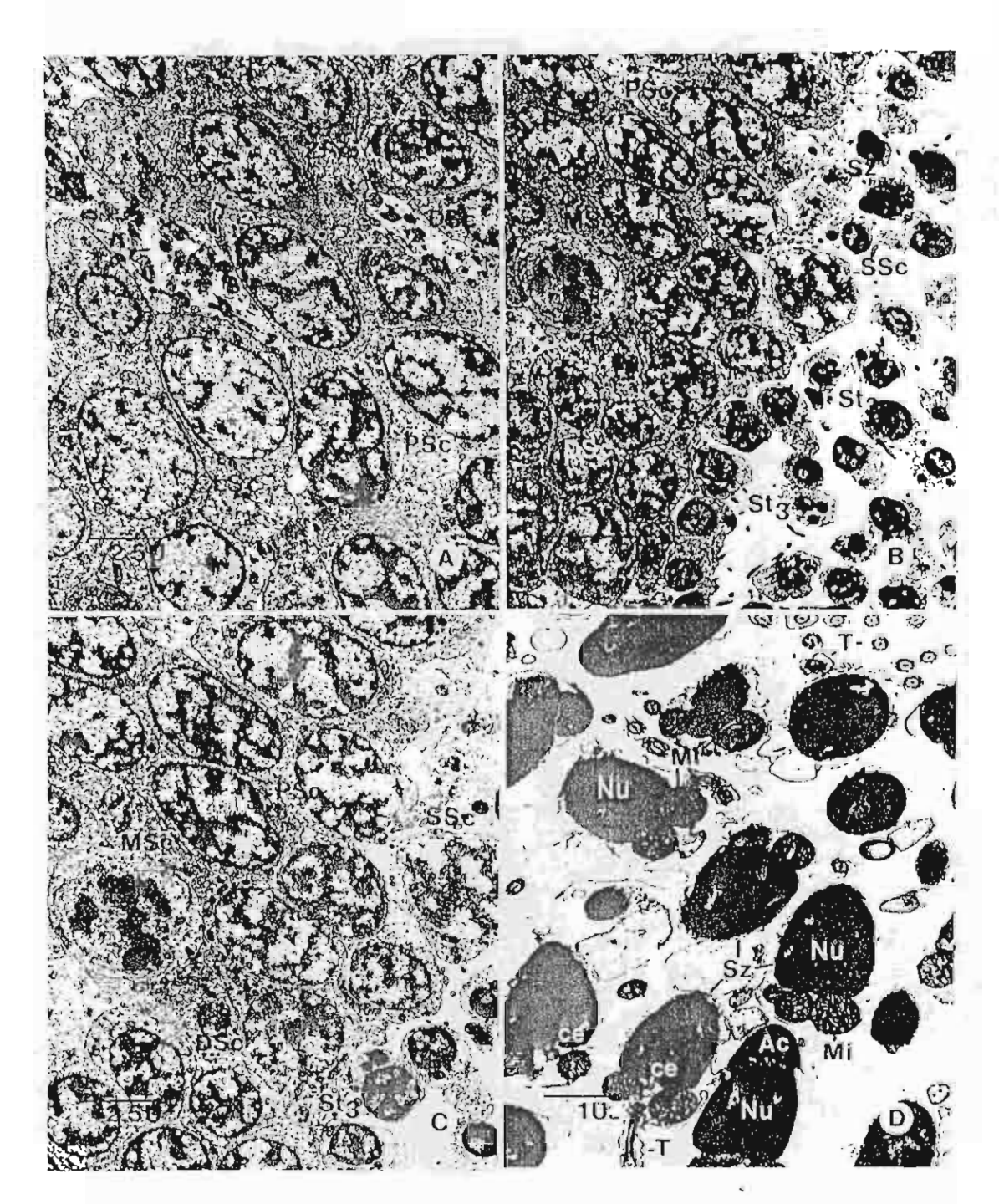


Fig.4 A-C) Electron micrographs showing various states of male garm cells, including leptotene (LSc), appearance (ZSc), pachytene (P.Sc), illufotene (DSc), recusality spectrum experimental (Ss).
 D) Spermatozoa exhibiting dense intefeos (Nu), acrosome (Ac), globular mitochondria (Mi), centrole (cc), and tails (T) with axonemal complexes.

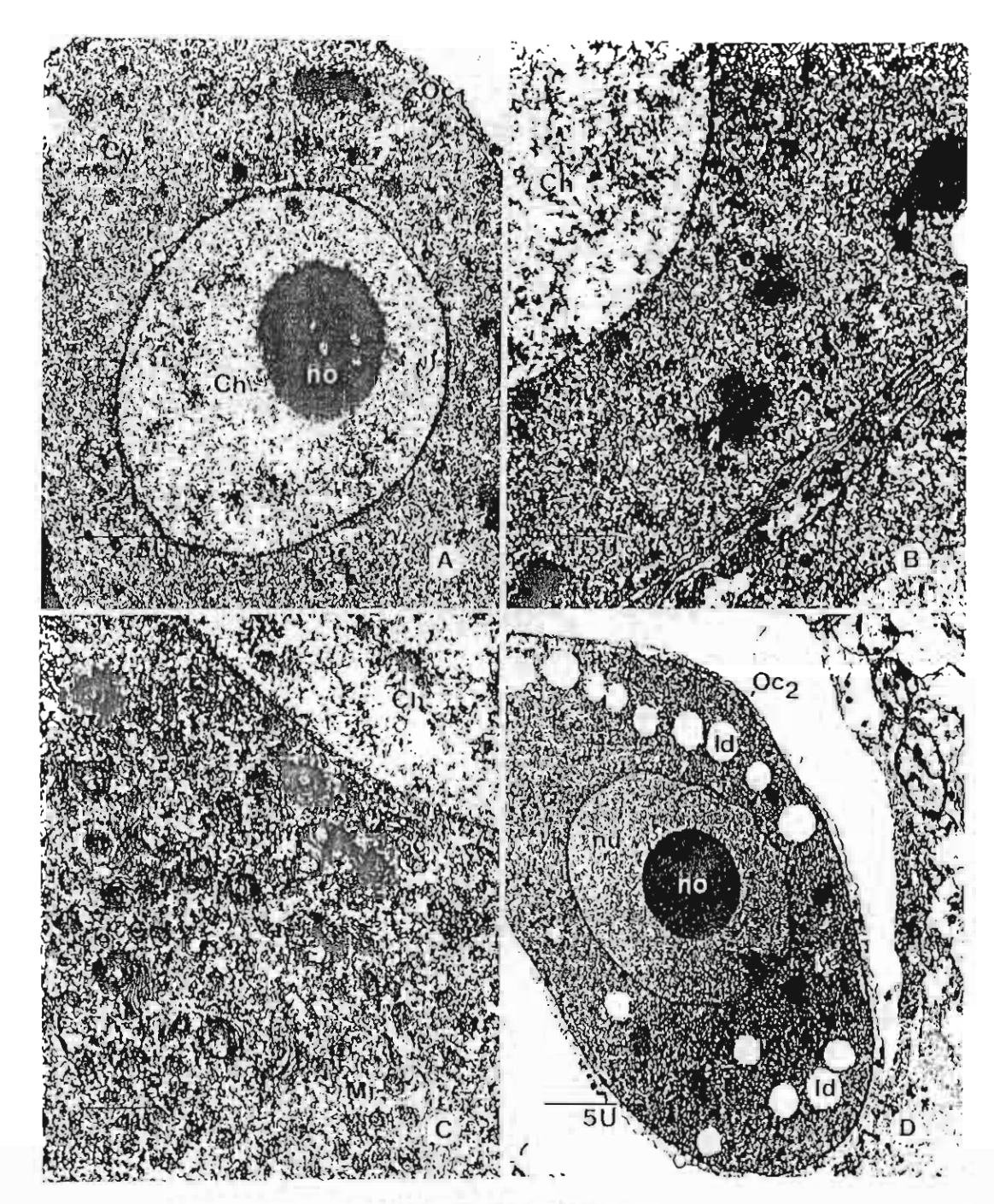


Fig.5 A,B) Early stage 1 oveyte (Oc1), exhibiting nucleus with lamphrish chromosomes (Ch), dense nucleolus (no), and eytoplasm (Cy) with aluminant ribosomes, some of which are apprepared in crystal-like bodies (arrows).

C) Late Oc1, exhibiting the extensive development of Golgi complexes (Gc) and mitochondria (Mi).

D) Stage II occyte (Oc2), exhibiting lipid droptets (Id), nucleus with uncoiled and clear chromatin and nucleolus (no).

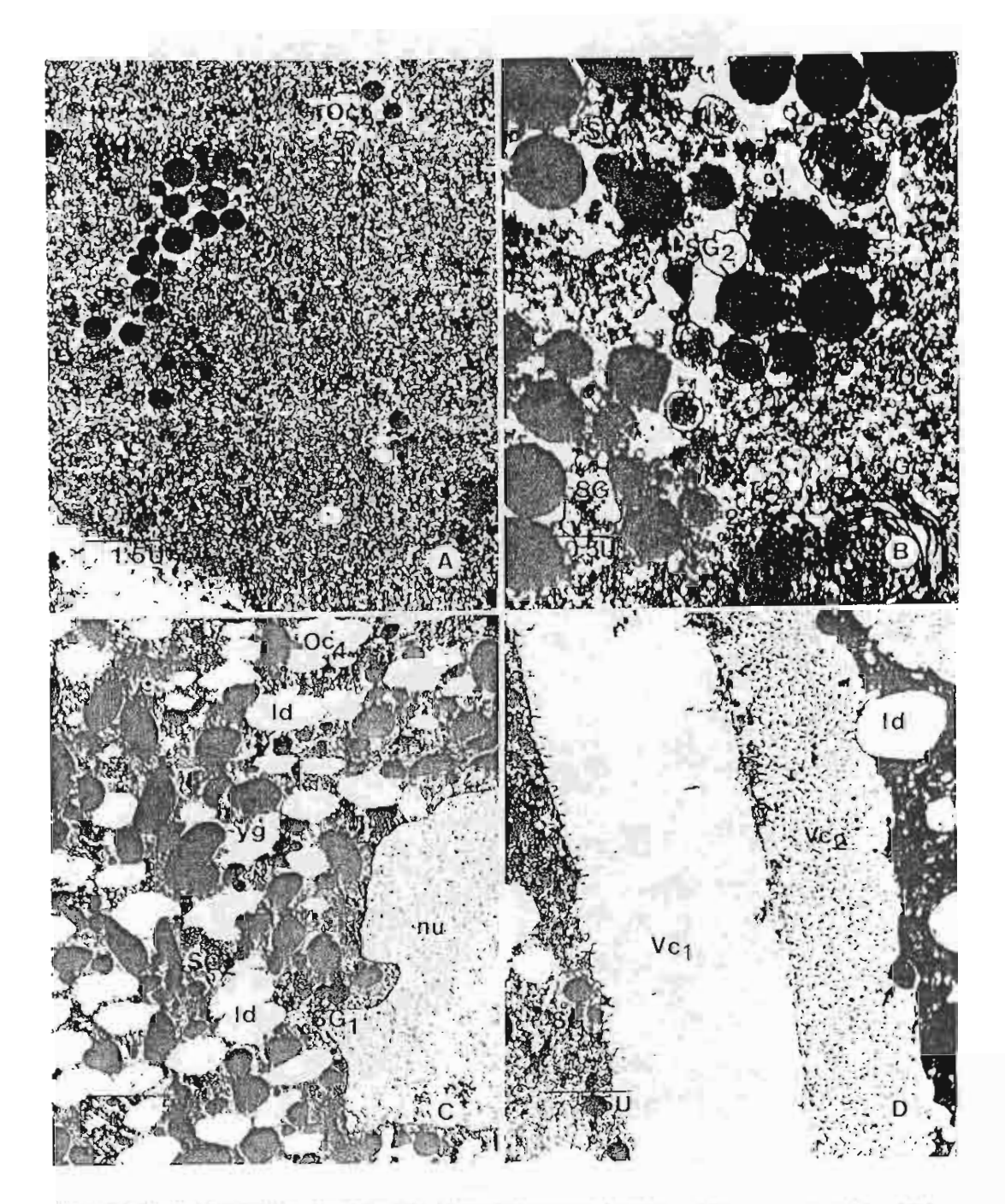


Fig.6 A,B) The cytoplasm of Oc<sub>2</sub> (A) and Oc<sub>3</sub> (B) exhibiting high concentration of dense jelly coat granules (SG<sub>3</sub>) and lighter control granules (SG<sub>3</sub>) around Golgi complexes (Ge).

- C) Fourth stage cocyte ( $O_{C_0}$ ) exhibiting very light nucleus ( $n_0$ ) due to completely uncoiled chromatin. The cytoplasm contains numerous large yolk granules ( $y_0$ ), small  $SG_1$  and  $SG_2$  granules
- D) The homogeneous jelly cont of  $Oc_4$  ( $Vc_1$ ) and fibrous jelly cont of  $Oc_5$  ( $Vc_2$ ). Notice the executosis of  $SG_4$  into jelly cont  $Vc_1$  (arrow)

#### DISCUSSION

Gonadal Structure and Classification of Cells in Gametogenesis

The first accounts of reproductive biology on an abalone species, 11. tuberculata, was published by Stephenson since 1924 (11), and Croft (12) in 1929, who showed that the basic framework of the gonads is composed of fibrous capsular and trabecular supports, from which germ cells appear to generate. Similar histological studies in other species were later performed by many investigators (13, 14, 15, 16, 17, 18, 19, 20, 21, 22). More recently, a fine structural study of the ovarian cells in the red abalone, II. rufescens, was also undertaken by Martin et al. (23). All these studies confirmed similar pattern of structural organization of the gonads; however, there are some disagreements on the classification of the stages of germ cells in the oogenetic and spermatogenic processes (15, 16, 18, 20). Utilizing a high resolution TEM to study the relative abundance of various organelles, particularly ribosomes and the development of rough endoplasmic reticulum and Golgi complexes in the cells, Martin et al. (23) suggested that there are 5 stages of female germ cells in H. rufescens, which they termed ongonium, presynthetic oocyte, synthetic oocyte, early postsynthetic oocyte and fully developed postsynthetic oocyte. We feel that the classification based on size alone, as adopted by many investigators, is not a good criterion for dividing cells in a single line of differentiation into various stages, because in reality these cells are undergoing continuous development. A better criterion would be to divide the cells according to the changes in histological and ultrastructural features which reflect the beginning of different synthetic activities in various developmental stages. In our study of H. asinina, we have used the following light and electron microscopic characteristics for dividing the stages of female germ cells: 1) the appearance of nucleus and nucleolus especially with regard to the uncoiling of chromatin, as reflected by the clarity of the two structures; 2) the clarity of nuclear membrane which is the result of the density difference between the condensed chromatin in the nucleus and the surrounding cytoplasm; 3) the basophilia or the bluishness imparted to the cytoplasm of the cells by basophilic dyes which reflect the abundance of ribosomes in the cytoplasm; 4) the presence of lipid droplets; 5) the development of secretory organelles particularly rough endoplasmic reticulum and Golgi complexes; 6) the occurrence of basophilic secretory granules including cortical granules, and eosinophilic yolk granules, and their relative abundance; and 7) the presence of jelly coat surrounding the egg cells. By

using these rather stringent morphological criteria, we have identified 5 stages of egg cells, starting from oogonia (Og) which are the smallest cells closely attached to the connective tissue trabecula. These cells could maintain a constant pool of early stem cells, particularly those that are clustered towards the capsular side of trabeculae. During the spent period when most mature oocytes are released from the ovary and the connective tissues of trabeculae are breaking down, these cells are the only remaining group of germ cells. The restoration of gonadal structure during proliferative phase is carried out by the regeneration of connective tissues of trabeculae and the proliferation of this pool of oogonia.

The first stage of oocytes (Oc1) including cells of different sizes ranging from 20-24 µm. The most pronounced characteristics that they exhibit is the increasing basophilia or bluishness of their cytoplasm. And because of the similar degree of density between the cytoplasm on one hand, and the partially condensed chromatin and dense nucleoplasm on the other, the outline of nuclear membrane could not be easily discerned under LM. The nucleolus, while present, is not outstanding. All Oc, are surrounded by a single layer of flat follicular cells. Under TEM we found that there is increasing amount of ribosomes which reflects the intense cytoplasmic basophilia. While ribosomes are rapidly synthesized during the early stage of Oct, definite surge in the number and degree of development of Golgi complexes and RER are observed only in late Oc1. These two subgroups of Oc, do not yet exhibit any secretory granules. Thus they may correspond to the presynthetic oocytes as described by Martin et al. (23), when cells are preparing themselves for the onset of synthetic activities.

Oc<sub>2</sub> is the stage that first shows the presence of lipid droplets in the less intense basophilic cytoplasm. Due to the decondensation of most chromatin, and the increased translucence of the nucleoplasm, the nuclear boundary could be clearly observed under LM. For similar reasons the nucleolus also becomes more distinct; and because of its enlargement the nucleolar activities for ribosomal synthesis is believed to be on the increase (24). Under TEM, a few definite SG<sub>1</sub> and SG<sub>2</sub> granules start to appear in this stage, by clustering around Golgi complexes. Thus Oc<sub>2</sub> could, represent the initial phase of synthetic activities when jelly coat (SG<sub>1</sub>) and cortical granules (SG<sub>2</sub>) are first synthesized.

Oc<sub>3</sub> is the stage which cosinophilic yolk granules first appear, and later is increasing in

number; hence rendering the cytoplasm of Oca more reddish in contrast to that of Oc2, while the basophilic or bluish SG granules are seen scattered evenly between yolk granules and lipid droplets. We believed, therefore, that this is the stage where there is intense synthetic activities, since under TEM numerous SG<sub>1</sub> and SG<sub>2</sub> as well as yolk granules appear in large numbers; particularly SG<sub>1</sub> and SG2 were seen concentrating around Golgi complexes. Oc; is still surrounded by a single layer of follicular cells, which by this time consists of several cells because of the increase in size of the cell. In addition, Oc3 is further detached from the connectives of trabeculae and assumes a pear or even tear-drop shape. The chromatin becomes completely eucliromatic and the nucleolus is enlarged further as its chromatin are almost completely uncoiled; this implies the active transcriptional as well as translational activities.

Oc4 is the stage where a thin jelly coat is first detectable, and it is sandwiched in-between the egg's cell membrane and the surrounding layer of follicular cells. Under LM the cytoplasm of Oca becomes increasingly cosmophilic and appears more reddish due to the staining of numerous yolk granules by eosin. While the jelly coat is intensely PAS positive, the yolk granules are completely PAS negative. The contrasting feature implies that there may be very little or no carbohydrate moieties in the yolk granules, while these are the major constituent of the jelly coat. Under TEM the cytoplasin of Oc4 is filled with SG1, SG2 and yolk granules, which reflect the near saturation of synthetic activities. The chromatin of Oc4, like that of Oc3, is completely in euchromatic state and the nucleolus is fully enlarged due to the complete uncoiling of its chromatin, and under LM it even appears cosinophilic. These indicate still high levels of both nuclear and nucleolar transcriptional activities. Another remarkable feature of Oca under LM is the appearance of a narrow bluish stripe in the cytoplasm just underneath the cell membrane, while the bluishness of the remaining mass of cytoplasm is much decreased in comparison to Oc2 and Oc3. This could be due to the high concentration of basophilic SG1 and SG2 granules which are translocated to this area as observed under TEM. Some of the more electron SG; granules are also seen exocytosed to the cell's periphery, and thus is believed to contribute material to the formation of the jelly coat. In contrast, SG2 contains more electron lucent material than SG<sub>1</sub>. They may be the actual cortical granules that are concentrated in the narrow cytoplasmic zone underneath the plasma membrane, and thus are kept in reserve for cortical reaction upon fertilization of the egg by the sperm.

Ocs is the stage where the jelly coat becomes uniformly thick and deprived of surrounding layer of follicular cells. Under TEM the jelly coat is transformed from homogeneous in Oc4 to fibrous structure in Oc5. There is no division of this cell coat into jelly and vitelline layers as reported in other species (25). Thus Oc<sub>5</sub> appears completely mature and is fully detached from the trabeculae. The absence of follicular cells might allow the detachment of Ocs into space between trabeculae and ready them for release from the ovary. From this appearance it could be speculated that the major roles of follicular cells are protective and helping to maintain the adherence between oocytes and trabecula connective tissue, while the former are undergoing maturation. In addition, follicular cells could be involved in nutritive function for opeytes, and their roles in synthesizing the jelly coat could not yet be ruled out. Under LM the cytoplasm of Ocs is laden with reddish yolk granules. Based on the size of these yolk granules there could be 2 subgroups of Ocs: one containing small granules of uniform size while the other contains very large granules, both of which appear very electron opaque under TEM. It is still not possible to confirm whether these are two separate stages of Ocs, or that the latter merely represent the final stage in which small yolk granules are coalesced to form larger ones. In any cases these two subgroups of Ocs should represent fully mature cells. In comparison to the work of Martin et al. (23), Oc4 could represented the early postsynthetic cells and Oc; late postsynthetic cells; even though, judging from ultrastructural features certain degree of synthetic activities must still be carried out in these cells.

Up to now most studies have not rigorously categorize various spermatogenic cells of Haliotis, apart from suggesting broadly that there are 4 stages, i.e., spermatogonia, spermatocytes, spermatids and spermatozoa (16, 18, 20). In the present study, the male germ cells in H. asinina could be classified into 13 specific stages according to the size, shape, appearance of chromatin and the presence or absence of nucleolus. Spermatogonium is the earliest cell whose nucleus contains almost all euchromatia which results in the nucleus being very clear and nucleolus is prominent. Spermatogonia divided mitotically to give rise to primary spermatocytes, which pass through 5 stages as in the first meiotic division of vertebrates' germ cells (26). These prophase cells exhibit different forms of chromatin condensation, beginning with small to larger blocks of heterochromatin that are evenly scattered throughout the nucleus in LSc and ZSc. Heterochromatin blocks transform to thread-like pattern that are increasing in thickness and length, and become more entwined in PSc and DSc.

Ŀ

3

0

C

Finally in diakinetic and MSc stages chromatin appears as pairs of chromatids that are translocated to the equatorial region. Secondary spermatocytes are quite numerous in comparison to those in vertebrates and they have heterochromatin that exhibit checker-board or XY-figure pattern.

Four stages of spermatids could be identified in H. asinina based on the nuclear size, shape and chromatin condensation. Under LM the first two stages exhibit finely granulated chromatin that appears homogeneous and evenly stained throughout the nuclei. Thus St, and St, could be distinguished by the difference in size (St. about 6 jum versus St2 about 4 jun), and by the denser nuclear material in St2. The latter is due to the reduction of nuclear volume which results in the closer packing of chromatin fibers, even though each fibers still maintain their width of 30 nm. In the third stage (St3) the chromatin fibers begins to be tightly wound together into large dense blocks. particularly along the nuclear envelope, leaving clear areas between the blocks. At this stage individual fiber increases in size to 40 nm. Eventually, the decrease in volume of nucleus and its more ellipsoid shape results in the total condensation of chromatin mass in St., and individual chromatin fiber is enlarged to 60 nm.

The two stages of spermatozoa are distinguished by their ellipsoid nuclei. Sz<sub>1</sub> also shows the initial formation of acrosome as a clear cap-like structure on one end of the nucleus, while exhibiting only short tail. Under TEM, there is the formation of axonemal complexes from centriolar pair that move to the neck area just distal to the nucleus. Later, three to five globular mitochondria become localized around the centrioles. In Sz<sub>2</sub> the nucleus is elongated further and chromatin appears completely dense with the outline of 60 nm fibers (or granules) barely discernible. Sz<sub>2</sub> exhibits a completely formed tail that is long and point outwards from each trabecula.

#### Reproductive Cycle

There have been a number of studies on the course of reproductive cycle in various abalone species by many investigators. The two methods that are frequently used for determining a reproductive cycle of a population are: 1) the measuring of the relative size of gonads with respect to the size of conical organ which is termed gonad indices (GI); and 2) the assessing of histological changes in the gonads (17, 27, 28, 29, 30). GI is not always a valid index for development of the gonads because GI only relates gonad area to constant parameters (e.g. the size of conical organ) of the animal, and it does not take variation in hepatopancreas size into account (18, 31). The

more precise index that can define of reproductive cycle better is the use of histological examination of gonad sections, which can give considerable details of cellular association and the time interval between successive phases (17). Many investigators, including Tomita (15, 16), Lee (32), Giorgi & DeMartini (33), Ault (30), classified the reproductive stages in various temperate species of Haliotis into 5 to 6 distinct phases which are more clearly defined in females. In the present study, these various phases were also observed in H. Histological examination of monthly samplings of the brooding stocks cultured in the land-based culture system reveal 5 distinctive gonadal patterns during the year, i.e., proliferative, premature, mature, spawning and spent phase.

Proliferative phase is characterized by the regeneration of gamete cells for the new cycle. The gonads contain mostly early stage germ cells in both sexes, such as Og, Oc, Oc2 in the ovary, and mainly Sg, PrSc without St and Sz in the testis. Giorgi & DeMartini (33) and Ault (30), on studying H. rufescens, found that the ovary contained primarily small oocytes usually lesser than 50 µm in diameter; while Tomita (15), on studying H. discus hannai, reported that there are mainly oogonia, yolkless and oil drop oocytes in this stage. Another remarkable features during this phase is the reciprocal relationship between the sizes of the gonads to the hepatopancreas, which is similar to that found in other Haliotid (13, 17). That is the hepatopancreas is relatively large when compared to the total area of conical organ. Boolootian et al. (13) also reported that, in H. cracherodii and H. rufescens, the size of hepatopancreas exhibits an inverse relationship to gonadal activity. During this phase, the hepatopancreas attains maximum size while the gonad activity is relatively quiescent. The precipitous drop in the size of hepatopancreas will occur during the subsequently phase when there is a rapid growth of the gonads. This implies that hepatopancreas may act as a nutrient storage that is necessary for gamete cells development; it becomes relatively depleted when the proliferation of gonad cells start to surge. Another remarkable histological features observed during this phase is the dilatation of the trabecular vessels which contain large amount of granular materials. This may represent the turgid state of the vessels that are supplying nutrients to the rapidly proliferating and growing gamete cells.

Premature phase is the period of rapid increase in numbers and sizes of gamete cells. The ovary contains predominantly Og,  $Oc_1$ ,  $Oc_2$  and  $Oc_3$ , which is similar to those reported in the premature stage of H. discus hannai (15, 34); while Sg, Sc and only few of St and Sz are evident in the

testis during this phase. Ault (30), in studying *H. rufescens*, also reported that there were numerous developing early germ cells in this stage. Hence the major events of development in this phase involve the rapid growth of the gonads due to fast proliferation of early germ cells.

Mature phase is characterized by a notable enlargement of the gonads which exhibit striking differences of color between both sexes: greenish in female and yellowish in male. The ovary contains mostly late stage germ cells, i.e., Oc, with widely scattered Oc; and the testis is mostly filled with St and Sz. Before spawning occurs, Oc, are detached from trabeculae and released into the gonadal lumen. During the rapid development of the testis, each trabecula is surrounded successively by a few rows of Sg, PrSc which are closely bound to trabecular connectives, and middle Sc, St appear further away, and Sz are completely detached from trabeculae. In comparison, during differentiation of Oc, to Oc, from Og, the cells move along the trabeculae from capsular side towards the hepatopancreas side, until Oc, become detached from trabeculae.

Spawning phase is the time when gravid abalone start to release their ripened gametes. The period of spawning is the most important criterion for success of reproduction of various abalone species reared in close aquaculture system (13, 14, 15, 16, 17, 18, 19, 29, 33, 35, 36, 37). From many previous studies, spawning periods have been found to vary considerably among various species of abalone, and from year to year according to geographical locations, and local environment, such as food supply, temperature and the day length (17, 34, 38, 39, 40, 41). Thus, some investigators (13, 36) have classified various Haliotid spp. into 3 groups according to their spawning season: those spawn during summer, those spawn during seasons other than summer, and those that exhibit yearround spawning. Earlier, Singhagraiwan & Doi (42) reported the spawning period of some wild broodstocks of 11. asinina to peak around October, while the pond-reared broodstocks could spawning throughout the year with several minor peaks during March through September. In contrast, the spawning period of H. asinina kept in land-based closed culture system in the present study occurs twice a year: around August to October and March to April in female, and around August to October and February to March in male. While this is the general pattern of spawning for most members of the population, some individual may show irregular

periodic spawning throughout the year, especially in males animals.

Spent phase is characterized by the lacking of gamete cells and the breakdown of connective tissue in the gonads, which is similar to that previously finding in H. rufescens (33). According to Shepherd & Laws (36), spent phase is expressed when there is a complete discharge of gamete cells following spawning. Giese (28) defined spent phase in marine invertebrates as a postspawning quiescent stage which is indistinguishable between male and female. In present study, it was observed that during the spent phase the gonads of H. asinina are greatly reduced in size and become creamy in color, and the sexes of animals cannot be In contrast, hepatopancreas is distinguished. relatively increased in size which may be filled up with food reserve. It was revealed that spent phase of H. asinina are observed usually around September to October and April to June in both sexes.

From the data collected during one year period, it could be concluded that the spawning of II. asinina reared in the closed culture system can occur at least twice yearly providing that the culturing condition and food supply are optimal. And that each reproductive cycle, consisting of 5 phases of development needs at least 5 to 6 months to complete itself.

#### **Development of Gonads**

In previous studies of the gonadal development in II. asinina, fecundity was observed in females with the shell length of at least 48 mm for the wild broodstock, and 44 mm of the hatchery-reared broodstock, which was about nine months old (43, 44). On the other hand, the mature gonad of males become obvious in animals with the shell length of at least 31 mm, which was about seven and a half months old (42, 43, 44). The data collected in the present study indicate the same Furthermore, detailed histological study indicated that definitive gonads become clearly separated from the hepatopanereas at 4 month, Testis and ovary could be distinguished by the present of their initial stages of germ cells as early as 5 month. Testis tends to reach maturity quicker than every at 6 to 7 months, the time at which St and Sz are found to be abundant. Ovary tends to mature later at 10 to 11 months when it starts to contain mature oocytes (Oc4 and Oc5). By 11 to 12 month both sexes of II. asinina assume their continuous reproductive cycles.

#### LITERATURE CITED

- Nateewathana A, Hylleberge J. A survey on Thai abalone around Phuket Island and feasibility study of abalone culture in Thailand. Thai Fish Gazette 1986;39:177-190.
- Tookvinart S, Leknim W, Donyadol Y, Preeda-Lampabutra Y, Perng mak P. Survey on species and distribution of abalone (Haliotis spp.) in Surajthani, Nakornsrithammaraj and Songkhla provinces. National Institute of Coastal Aquaculture, Department of Fisheries, Ministry of Agriculture and Cooperatives, Thailand, 1986. Technical Paper No. 1/1986.
- Nateewathana A, Bussarawit S. Abundance and distribution of abalones along the Andaman Sea Coast of Thailand. Kasetsart J (Nat Sci) 1988;22:8-15.
- Singhagraiwan T, Sasaki M. Breeding and early development of the donkey's ear abalone, Haliotis asinina Linne. Thai Mar Fish Res Bull 1991a;2:83-94.
- Singhagraiwan T, Sasaki M. Growth rate of donkey's ear abalone, *Haliotis asinina* Linne, cultured in tank. Thai Mar Fish Res Bull 1991b;2:95-100.
- Kakhai N, Petjannat K. Survey on species and broodstock collection of abalone (Haliotis spp.) in Chon-buri, Rayong and Trad provinces. Aquaculture Station, Coastal Aquaculture Division, Department of Fisheries, Ministry of Agriculture and Cooperatives, Thailand, 1992. Technical Paper No.6/1992.
- Singhagraiwan T, Doi M. Seed production and culture of a tropical abalone, Haliotis asinina Linne. The Eastern Marine Fisheries Development Center, Department of Fisheries, Ministry of Agriculture and Cooperatives, Thailand, 1993.
- Sungthong S, Ingsrisawang V, Fujiwara S. Study on the relative growth of abalone, *Haliotis* asinina Linne, off Samet Island. Thai Mar Fish Res Bull 1991;2:120.
- 9.Bussarawit S, Kawintertwathana P, Nateewathana A. Preliminary study on reproductive biology of the abalone (Haliotis varia) at Phuket, Andaman Sea Coast of Thailand. Kasetsart J (Nat Sci) 1990;24:529-39.
- 10.Jarayabaand P, Jew N, Manasveta P, Choonhabandit S. Gametogenic cycle of abalone *Italiotis* ovina Gmelin 1791 at Khangkao Island, Chon-buri province. Thai J Aqua Sci 1994;1:43–42.
- Stephenson TA. Notes on Haliotis tuberculata. J Marin Biol Assoc UK, 1924;13:480-495.
- Croft DR. Haliotis, L.M.B.C. mem: Liverpool University Press, 1929:174p.

- Boolootian RA, Farmanfarmaian A, Giese AC.
   On the reproductive cycle and breeding habits
   of two western species of *Haliotis*. Biol Bull
   1962;122:183-93.
- 14. Newman GG. Reproduction of the South African abalone *Haliotis midae*. Division of Sea Fisherics, Republic of South Africa, 1967. Investigational Report No. 64:24p.
- 15. Tomita K. The maturation of the ovaries of the abalone, Haliotis discus hannai Ino, in the Rebun Island, Hokkaido, Japan. Sci Rep Hokkaido Fish Exp Sta 1967;7:1-7.
- 16. Tomita K. The testis maturation of the abalone, Huliotis discus hannai luo, in the Rebun Island, Hokkaido, Japan. Sci Rep Hokkaido Fish Exp Sta 1968;9:56-61.
- 17. Webber IIH, Giese AC. Reproductive cycle and gametogenesis in the black abalone *Haliotis* cracherodii (gastropoda: prosobranchiata). Mar Bio 1969;4:152-9.
- 18. Young JS, DeMartini JD. The reproductive cycle, gonadal histology and gametogenesis of the red abalone, *Haliotis rufescens* (Swainson). Calif Fish and Game 1970;56:298-309.
- 19.Harrison AJ, Grant JF. Progress in abalone research. Tasm Fish Res 1971;5:1-10.
- Takashima F, Okuno M, Nichimura K, Nomura M. Gametogenesis and reproductive cycle in Haliotis diversicolor diversicolor Reeve. J Tokyo Univ Fish 1978;1:I-8.
- 21. Brickey BE. The histological and cytological aspects of oogenesis in the California abalones. (M.S. Thesis) Long Beach (CA): California State University, 1979.
- 22. Tutschultz T, Connell JH. Reproductive biology of three species of abalone (*Haliotis*) in southern California. The Veliger 1981; 23:195-206.
- 23. Martin GG, Romero K, Miller-Walker C. Fine structure of the overy in the red abalone *Haliotis rufescens* (Mollusca: gastropoda). Zoomorphology 1983;103:89-102.
- 24. Schwarzacher HG, Wachtfer F. The nucleolus.

  Anat Embryol 1993;188:515-36.
- Monzingo NM, Vacquier VD, Chandler DE. Structural features of the abalone egg extracellular matrix and its role in gamete interaction during fertilization. Mol Reprod Dev 1995;41:493-502.
- 26.Courot M, Hochereau-de Reviers M-T, Ortavant R. Spermatogenesis. In: Johnson AD, editor. The Testis. Academic Press: New York, 1970:399p.

- 27 Hahn KO. Gonad reproductive cycle. In: Hahn KO, editor. Handbook of culture of abalone and other marine gastropods. CRC Press: Boca Raton (FL), 1989:13-39.
- 28. Giese AC. Comparative physiology: annual reproductive cycle of marine invertebrates. Ann Rev Physio 1959;21:547-76.
- Grant A, Tyler PA. The analysis of data in studies of invertebrate reproduction. I. Introduction and statistical analysis of gonad indices and maturity indices. Int J Invertebr Reprod 1983;6:259.
- Ault J. Some quantitative aspects of reproduction and growth of red abalone, Haliotis rufescens Swainson. J World Maricult Soc 1985;16:398-425.
- 31. Hahn KO. The reproductive cycle and gonadal histology of the pinto abalone, *Haliotis kamtschatkana* Jonas, and the flat abalone, *Haliotis walallensis* Steams. Adv Invertebr Reprod 1981;2:387.
- 32. Lee TY. Histological study on gametogenesis and reproductive cycle of the Korean Coasts. Bull Pusan Fish Coll 1974;14:55.
- 33. Giorgi AE, DeMartini JD. A study of the reproductive biology of the red abalone, Haliotis rufescens Swainson, near Mendocino, California. Calif Fish and Game 1977;63:80-94.
- 34. Mugiya Y, Kobayashi J, Nishikawa N, Motoya S. Gonadal maturation in the abalone, *Haliotis discus hannai* at Taisei, Hokkaido. Bull Fac Fish Hokkaido Univ 1980;31:306-13.
- Poore GCB. Ecology of New Zealand abalones, Haliotis species (mollusca: gastropoda). New Zealand J Mar Freshwat Res 1973;6:534-59.

- Shepherd SA, Laws HM. Studies on southern Australian abalone (Genus Haliotis). II. Reproduction of five species. Aust J Mar Freshwat Res 1974;35:49-62.
- Girard A. La reproduction de l'ormeau *Italiotis* tuberculata L. Rev Trav Inst Peches Marit 1972;36;163-84.
- Cox KW. Review of the abalone of California. Calif Fish and Game 1962;46:381-406.
- Uki N, Kikuchi S. Regulation of maturation and spawning of an abalone, Haliotis (Gastropoda) by external environmental factors. Aquaculture 1984;39:247-61.
- Kinne O. Temperature. In: Kinne O, editor.
   Marine ecology: A comprehensive integrated treatise on life in oceans and coastal waters.
   Vol. 1. Wiley-Interscience: London, 1970; 407-514.
- Shepherd SA. Studies on southern Australian abalone (Genus Haliotis). I. The ecology of five sympatric species. Aust J Mar Freshwat Res 1973;24:217-57.
- 42. Singhagraiwan T, Doi M. Spawning pattern and fecundity of the donkey's ear abalone, *Haliotis asinina* Lime, observed in captivity. Thai Mar Fish Res Bull 1992;3:61-9.
- Singhagraiwan T. The experiment on breeding and nursing of Donkey's ear abalone (Haliotis asinina Linne). The Eastern Marine Fisheries Development Center, Department of Fisheries, Ministry of Agriculture and Cooperatives, Thailand, 1989a. Technical Paper No.21/1989a.

a

5

a

P

n

d

(l si

m

de Ni lia Sp (S pro ou or pro ab pro be-

44. Singhagraiwan T. Study on growth rate of donkey's ear abalone (Haliotis asinina Linne) The Eastern Marine Fisheries Development Center, Department of Fisheries, Ministry of Agriculture and Cooperatives, Thailand, 1991. Technical Paper No.28/1991. REPRINTED FROM:

2nd Congress of the

Federation of Immunological Societies of Asia-Oceania

Bangkok (Thailand), January 23-27, 2000

# **Editors**

STITAYA SIRISINHA SANSANEE C. CHAIYAROJ PRAMUAN TAPCHAISRI



MONDUZZI EDITORE

INTERNATIONAL  $ar{P}$ ROCEEDINGS  $ar{D}$ IVISION

# Molecular Cloning and Characterization of Antigen Encoding Genes from *Fasciola Gigantica*

R. Grams, S. Vichasri-Grams\*, P. Sobhon\*\*, E.S. Upatham\*\*\* and V. Viyanant\*

Faculty of Allied Health Sciences, Thammasat University, Pathum Thani, Thailand \* Department of Biology

\*\* Department of Anatomy

Faculty of Science, Mahidol University, Bangkok, Thailand

\*\*\* Department of Biology, Faculty of Science, Mahidol University, Bangkok, and Faculty of Science, Burapha University, Chonburi, Thailand

# **Summary**

Several homologous cDNAs encoding known antigenic proteins of Fasciola hepatica were cloned by RT-PCR from Fasciola gigantica. Analyses were done to determine DNA/amino acid sequences and to study the expression at the RNA level by Northern and RNA in situ hybridization. Southern hybridization was used to analyze the number of gene copies present in the genome for each of the studied genes. Here, we present preliminary sequence data obtained for fatty acid binding protein, glutathione S-transferase and cathepsin L. The nucleotide sequences were submitted to Genbank (AF112566, AF112567, AF112568)

### Introduction

Fasciola gigantica is a common parasite of cattle in Thailand. It causes severe disease and important economic losses in animal husbandry (SRIHAKIM and PHOLPARK, 1991). Therefore, this molecular study was done as a starting project for future work on diagnosis and vaccination of fascioliasis in cattle in Thailand. Three proteins under investigation for their diagnostic and protective properties in Fasciola

were choosen for this study. These proteins are cathepsin L (CatL), fatty acid binding protein (FABP) and glutathione S-transferase (GST) (ESTUNINGSIH et al., 1997; SPITHILL et al., 1997). GSTs are a major class of detoxification enzymes (MANNERVIK, 1985). CatL belongs to the group of cysteine proteases. F. hepatica CatL was shown to prevent the adherence of eosinophils to newly excysted juveniles by its ability to cleave host immunoglobulin. Therefore, this protease may have an important biological function in immune evasion in Fasciola (CARMONA et al., 1993; SMITH et al., 1993, 1994). FABPs are essential molecules in platyhelminthes, as these parasites are unable to synthesize most of their own lipids (MCMANUS and BRYANT, 1986).

# Materials and Methods

Total RNA from adult Fasciola gigantica was extracted by the TRIZOL method, following instructions given in the manual (Life Technologies). One microgram each of total RNA was reverse transcribed by Superscript II RT (Life Technologies) using gene-specific reverse primers (CatL-R: 5'-TCA CGG AAA TCG TGC CAC C-3', FABP-R: 5'-ACG CTT TGA GCA GAG TGG TC-3', GST-R: 5'-TCA AGC CGG TGC AGC GTC TC-3). The RT-products were used to amplify coding gene fragments by a standard Tag-based PCR setup (30 cycles at 55°C, 72°C, 92°C, one min each step). Beside the indicated reverse primers, three gene-specific forward primers were used (CatL: 5'-ATG CGA TTG TTC ATA TTA GC-3', FABP-F: 5'-ATG GCT GAC TTT GTG GGT TC-3', GST-F: 5'-ATG CCA GCC AAA CTC GGA TA-3'). The RT-PCR products were size-separated in agarose gels, cut and purified from the gel (Gel Extraction Kit, QIAGEN) and subcloned into either the T-Easy plasmid vector (Promega) or the T-extended EcoR V site of the pBluescript SK plasmid vector (Stratagene). Plasmid DNA was prepared using a plasmid miniprep kit (QIAGEN). For DNA sequencing, the services of NSTDA Bioservice Unit, Thailand and MWG AG Biotech, Germany were used.

## Results

The RT-PCR resulted in the generation of one prominent DNA fragment in each amplification experiment. Sequence analysis of the 981 bp CatL RT-PCR product showed this DNA fragment to be a closely related homolog of *Fasciola* sp. CatL S70380 (YAMASAKI and AOKI, 1993). At the DNA level identity is 98.7% (10 mismatches, one deletion of a three base pair segment). The deduced amino acid sequences are 98.5% identical (5 mismatches/326 residues, Figure 1A). The FABP RT-

A		
	${\tt MRLFILAVLTVGVLGSNDDLWHQWKRMYNKEYNGADDEHRRNIWEENVKHIQEHNLRHDL}$	60
Fs C:	V	60
		100
Fg C:	GLVTYTLGLNQFTDMTFEEFKAKYLTEMPRASDILSHGIPYEANNRAVPDKIDWRESGYV	120
Fs C:	L	120
Fq C:	TELKDQGNCGSCWAFSTTGTMEGQYMKNERTSISFSEQQLVDCSGPWGNMGCSGGLMENA	180
Fs C:	v	180
	•	0.40
	YEYLKQFGLETESSYPYTAVEGQCRYNRQLGVAKVTDYYTVHSGSEVELKNLVGAEGPAA	
Fs C:		240
Fa C:	VAVDVESDFMMYSGGIYQSRTCSSLRVNHAVLAVGYGTQGGTDYWIVKNSWGSSWGERGY	300
	IRMVRNRGNMCGIASLASLPMVARFP	326
Fs C:		325
В		
Fq F:	MADFVGSWKYGDSENMEAYLKKLGISSDMVDKILNAKPEFTFTLEGNQMTIKMVSSLKTK	60
Fh F:	HK	60
-	ITTFTFGEEFKEETADGKTAMTTVTKDSESKMTQVITGPEYTTHVVREVVGDKMIATWTV	
rn r:	EPKVKIKCI.E	120
Fq F:	GDVKAVTTLLKA	132
_		132
C		
C		
-	MPAKLGYWKIRGLQQPVRLLLEYLDEEYEEHLYGRDDREKWLGDKFNMGLDLPNLPYYID	60 60
rn G:		60
Fg G:	DKCKLTQSVAIMRYIADKHGMLGSTPEERARVSMIEGAAMDLRMGFVRVCYNPNFEEVKG	120
_	K	
_	DYLKELPKTLKMWSDFLGDRQYLTGSSVSHVDFMVYEALDCIRYLAPQCLNDFPKLKEFK	
rn G:	TNHP	180
Fa G:	SRIEDLPKIKAYMESEKFIKWPLNSWTASFGGGDAAPA	218
-	I	218

Figure 1: Alignments of the deduced CatL (A), FABP (B) and GST (C) amino acid sequences of F. gigantica (Fg), F. hepatica (Fh) and Fasciola sp. (Fs).

PCR product is 397 bp in length. Identity with the homologous gene of *F. hepatica* M92291 is 94.5% (20 mismatches, (HILLYER, 1995)). The deduced amino acid sequences are 89.4% identical (14 mismatches /132 residues, Figure 1B). The GST RT-PCR product is 657 bp in length. The

closest match in the Genbank is M77682, encoding a 26 kDa GST from *F. hepatica* (PANACCIO *et al.*, 1993). Identity of the DNA sequences is 97.3% with 18 mismatches in 657 bp. The deduced amino acid sequences are 95% identical (11 mismatches/207 residues, Figure 1C).

#### **Conclusions**

The obtained results show that the analyzed genes in Fasciola gigantica are closely related to the homologous genes of Fasciola hepatica. Detailed sequence analysis and additional molecular data on these genes, obtained by Southern, Northern and RNA in situ analysis will be published elsewhere.

# Acknowledgements

This work was supported by grants from the National Center for Genetic Engineering and Biotechnology (NSTDA, BT-B-06-2B-14-004) Thailand to V. Viyanant and the Thailand Research Fund (TRF, Senior Scholar Fellowship) to P. Sobhon.

#### References

- CARMONA, C., DOWD, A.J., SMITH, A.M., DALTON, J.P., Cathepsin L proteinase secreted by *Fasciola hepatica in vitro* prevents antibody-mediated eosinophil attachment to newly excysted juveniles, Mol. Biochem. Parasitol., 62, 9–17, 1993.
- ESTUNINGSIH, S.E., SMOOKER, P.M., WIEDOSARI, E., WIDJAJANTI, S., VAIANO, S., PARTOUTOMO, S., SPITHILL, T.W., Evaluation of antigens of *Fusciola gigantica* as vaccines against tropical fasciolosis in cattle, Int. J. Parasitol., 27, 1419–1428, 1997.
- HILLYER, G.V., Comparison of purified 12 kDa and recombinant 15 kDa Fasciola hepatica antigens related to a Schistosoma mansoni fatty acid binding protein, Mem. Inst. Oswaldo Cruz, 90, 249-253, 1995.
- MANNERVIK, B., The isoenzymes of glutathione transferase, Adv. Enzymol. Relat. Areas Mol. Biol., 57, 357-417, 1985.
- MCMANUS, D.P. and BRYANT, C., Biochemistry and physiology of *Echinococcus*, in THOMPSON, R.C.A. (ed.), The Biology of *Echinococcus* and Hydatid Disease. George Allen and Unwin Ltd, London, pp. 114–136, 1986.
- PANACCIO, M., WILSON, L.R., CRAMERI, S.L., WIJFFELS, G.L., SPITHILL, T.W., Molecular characterization of cDNA sequences encoding glutathione S-transferases of *Fasciola hepatica*, Exp. Parasitol., 77, 385, 1993.
- SMITH, A.M., DOWD, A.J., HEFFERNAN, M., ROBERTSON, C.D., DALTON, J.P., *Fasciola hepatica*: a secreted cathepsin L-like proteinase cleaves host immunoglobulin, Int. J. Parasitol., 23, 977–983, 1993.

- SMITH, A.M., CARMONA, C., DOWD, A.J., MCGONIGLE, S., ACOSTA, D., DALTON, J.P., Neutralization of the activity of a *Fasciola hepatica* cathepsin L proteinase by anti-cathepsin L antibodies, Parasite Immunol., 16, 325–328, 1994.
- SPITHILL, T.W., PIEDRAFITA, D., SMOOKER, P.M., Immunological approaches for the control of fasciolosis, Int. J. Parasitol., 27, 1221–1235, 1997.
- SRIHAKIM, S. and PHOLPARK, M., Problem of fascioliasis in animal husbandry in Thailand, Southeast Asian J. Trop. Med. Public Health, 22 Suppl, 352–355, 1991.
- YAMASAKI, H. and AOKI, T., Cloning and sequence analysis of the major cysteine protease expressed in the trematode parasite *Fasciola* sp, Biochem. Mol. Biol. Int., 31, 537–542, 1993.

REPRINTED FROM:

2nd Congress of the

Federation of Immunological Societies of Asia-Oceania

Bangkok (Thailand), January 23-27, 2000

**Editors** 

STITAYA SIRISINHA SANSANEE C. CHAIYAROJ PRAMUAN TAPCHAISRI



MONDUZZI EDITORE

International Proceedings Division

# Development of Immunodiagnosis for Fasciola Gigantica

P. Sobhon, V. Viyanant, E.S. Upatham, S.V. Grams,

P. Ardseungnoen, D. Krailas, W. Khawsuk, K. Chaithirayanon,

S. Sriburee, A. Meepool, C. Wanichanon, T. Chompoochan\*,

S. Thammasart\* and P. Prasitirat\*

Faculty of Science, Mahidol University, Bangkok, Thailand
\* Institute of Animal Health and Production, Livestock Department
Ministry of Agriculture and Cooperatives, Bangkok, Thailand

# Summary

Major antigens of adult *F. gigantica* have been identified by immunoblotting at molecular weights 66, 58, 54, 28.5 and 27-26 kD. Monoclonal antibodies (MoAb) against antigens at 66, 28.5, 27-26 kD have been produced; and MoAb against 66 and 28.5 kD showed more specificities while MoAb against 27-26 kD tended to have higher cross reactions with antigens from other trematode parasites. The tissue sources of these antigens have been studied by microscopic immunolocalization: 66, 58, 54 and 28.5 kD were associated with the surface membrane, tegument and tegument cells, while 27-26 kD were associated with the caecal epithelium.

# Introduction

In tropical region, including Thailand, fasciolosis is one of the major animal diseases due to infection by *Fasciola gigantica*. Infected animals exhibit decreased meat, wool production, growth rate, fecundity, and increased mortality in highly infected cases. There is a wide spread of fasciolosis in Thailand with the highest prevalent rate in the north-east and north, and the lowest in the south (24-4%). The disease can also cross-infect human, and the incidents have been reported in many parts of the world, with an estimation that as many as 17 million people are

infected worldwide. Chemotherapy and vector control have been used to control the infection. However, there have been reports on the emergence of drug-resistant parasites; and despite these control measures there is always a certain level of persistent endemic infection. Hence, there is much need for sensitive and specific methods of immunodiagnosis for monitoring the infection. Moreover, preventive measure through the development of vaccines that can confer long term protection for the animals may be the best solution. In the present report we have identified and localized candidate antigens of tegumental and caecal origins which may have immunodiagnostic and vaccine potentials.

## **Materials and Methods**

Major antigens in surface-tegument (ST) and excretory-secretory (ES) antigens of adult *F. gigantica* were characterized by immunoblotting using cow-infected serum (CIS) as probe<sup>3</sup>. Monoclonal antibodies (MoAbs) against these antigens were produced by hybridoma technology, and their specificities tested by immunoblotting against ST and ES antigens. These MoAbs were used to localize corresponding antigens in parasite's tissues by immunofluorescence. Cross reactions of these MoAbs against antigens from other trematode parasites (*S. spindale*, *S. mansoni*, *S. mekongi* and *Paramphistomum* spp.) were measured by ELISA.

# Results

Identification of antigen molecules and specificities of MoAbs

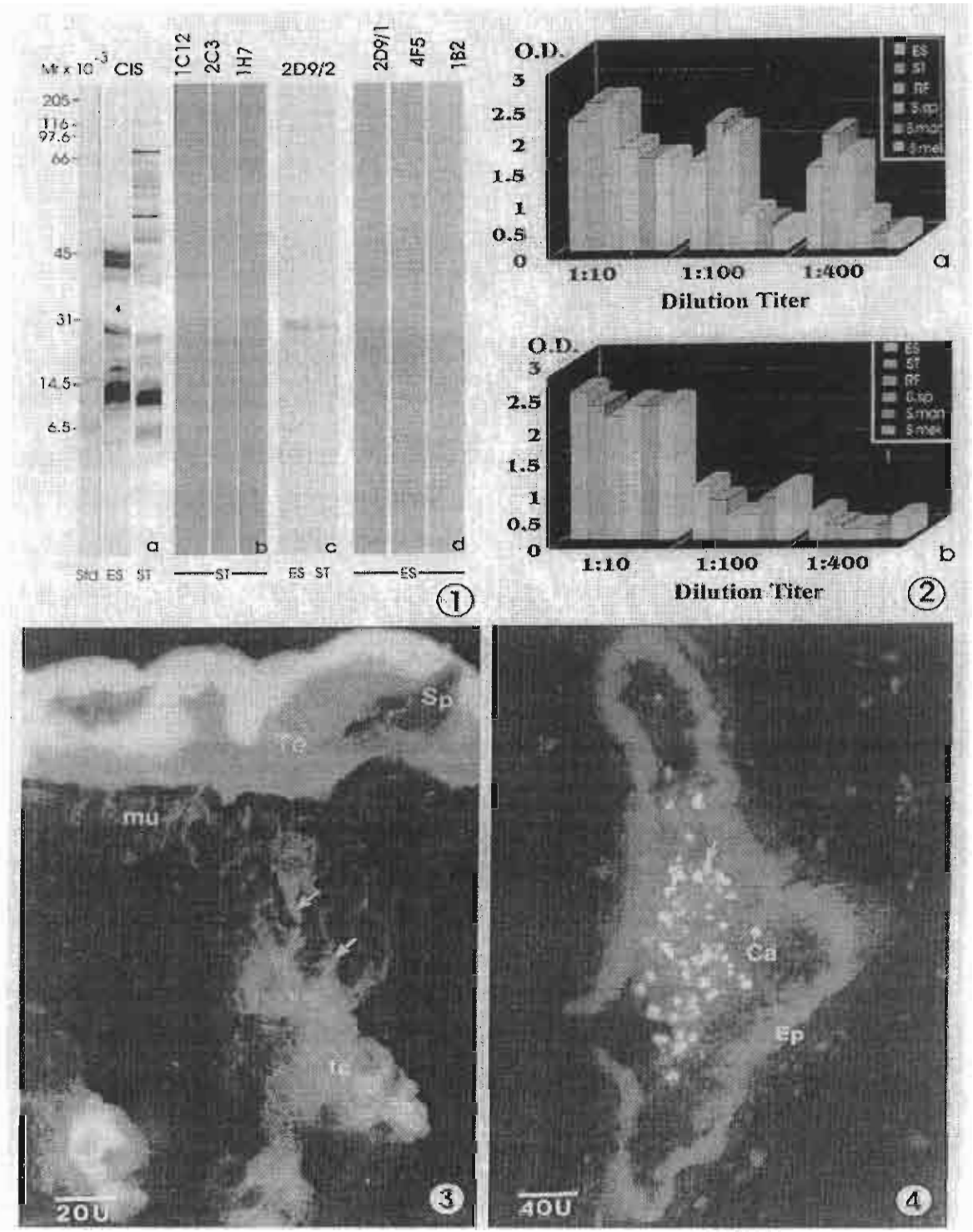
The result of immunoblotting between ST and ES antigens with CIS indicated the presence of seven major immunogenic bands at molecular weights 97, 66, 58, 54, 28.5 and 27-26 kD, respectively (Figure 1a).

# MoAbs reacting against surface-tegument (ST) antigens

Three stable clones of hybridomas were obtained, namely, 1C12, 2C3 and 1H7, which were IgM class; and all reacted with 66 kD band from ST-antigens as shown by immunoblotting (Figure 1b). These MoAbs were tested for cross reactivities by ELISA, and it was found that all three cross-reacted to varying degrees with the panel of antigens from four trematode species as already mentioned. However, significant reductions of their cross-reactivities were observed when these MoAbs were diluted to 1:100 and 1:400 (Figure 2a).

# MoAbs reacting against excretory-secretory (ES) antigens

MoAb against ES antigens were characterized by immunoblotting to react with 58, 54, 28.5 and 27-26 kD antigens (Fig. 1c, d). Of these the



Figures 1) Immunoblotting patterns of adult F. gigantica ES and ST antigens as detected by cow infected serum (CIS) (a), MoAbs against 66 kD (b), 28.5 kD (c), and 27-26 kD (d). 2) Cross reactivities of MoAb 1C12 (a) and 2D9/1 (b) with antigens from F. gigantica ES and ST fractions, Paramphistomum spp. (RF), S. spindale (S.sp), S. mansoni (S.man) and S. mekongi (S.mek). 3) Immuno-fluorescence localization of 28.5 kD antigen in adult F. gigantica tegument (Te), tegument cells (tc) and their processes by MoAb 2D9/2. 4) Localization of 27-26 kD antigens in the caecal epithelium (Ep) and lumen (Ca-arrow) by MoAb 2D9/1.

most reactive are MoAb against bands at 28.5 (clone 2D9/2) and 27-26 kD (clone 2D9/1 and 4F5). When the cross reactions with other trematodes' antigens were tested, MoAb against 27-26 kD show rather high cross reactivities at the dilution of 1:100 and 1:400 when compared to MoAb against 66 and 28.5 kD (Fig. 2b). MoAb against antigens at 58 and 54 kD were comparatively weak, hence they had not been studied further.

# Localization of antigens by monoclonal antibodies

# Tegumental antigens at 66, 28.5 kD

In adult and juvenile parasites, the immunostainings, using MoAbs against 66 and 28.5 kD antigens as probes, were detected in the tegument, especially at its outer rim, while spines were not stained. The intense staining also appeared in the tegumental cells lying beneath the subtegumental muscle layers, and their numerous processes running between muscle cells towards the tegument (Fig. 3). In addition, epithelia lining various parts of the digestive tract, such as, oral sucker, buccal tube, pharynx, esophagus, parts of the digestive tract proximal to caecal bifurcation were also intensely stained. In contrast, distal parts of the digestive tract lined by the caecal-type epithelium, muscle, and parenchyma cells were not stained. Furthermore, these monoclonal antibodies gave strong stainings of tegumental epithelium lining both male and female genital canals of the reproductive system.

In metacercariae, the two groups of MoAbs gave similar staining patterns. The main sites for immunostainings were the narrow tegument that lay underneath the inner cyst wall, and the finely granular cytoplasm of tegumental cells. The epithelium lining of oral and ventral suckers, which were the continuation of the tegument, were also intensely stained.

# Caecal antigens at 27-26 kD

MoAb 4F5 and 2D9/1, which reacted specifically with the ES antigens at 27-26 kD, showed staining in the epithelium lining of the adult and juvenile's caeca distal to the caecal bifurcation. The cytoplasm of these cells were moderately but evenly stained, while the nuclei were not. Intense staining was also observed in the caecal lumen, where food materials were mixed with the secreted enzymes (Fig. 4). These monoclonal antibodies did not stain corresponding tissues of metacercariae.

# **Conclusions**

MoAbs against ST and ES antigens of F. gigantica at 66, 28.5 and 27-26 kD were produced. From immunolocalization studies, 66 and 28.5 kD antigens were associated with the tegument, tegument cells, and surface membrane of all stages of the parasites, while 27-26 kD antigens

were associated with caecal epithelium of adult and late juvenile parasites only. When tested against antigens from other trematodes (*Paramphistomum* spp., *S. spindale*, *S. mansoni*, *S. mekongi*) MoAb against 66, 28.5 kD showed less cross reactivities than 27-26 kD antigens. Hence these antigens have potential for immunodiagnosis.

# Acknowledgements

This study was supported by grants from the Thailand Research Fund (Senior Research Scholar Fellowship to P. Sobhon) and from National Center for Genetic Engineering and Biotechnology, NSTDA (to V. Viyanant).

### References

- 1. SUKHAPESNA, V., TUNTASUVAN, D., SARATAPHAN, N. AND IMSUP, K. A study on the prevalence of liver fluke infection in cattle and buffaloes in Thailand. *J Thai Vet Med Assoc*, 40: 13-19, 1989.
- 2. SOBHON, P., ANANTAVARA, S., DANGPRASERT, T., VIYANANT, V., KRAILAS, D., UPATHAM, E.S., WANICHANON, C. AND KUSAMRAN, T. Fasciola gigantica: studies of the tegument as a basis for the developments of immunodiagnosis and vaccine. Southeast Asian J Trop Med Pub Hlth, 29: 387-400, 1998.
- 3. SOBHON, P., ANANTAVARA, S., DANGPRASERT, T., MEEPOOL, A., WANICHANON, C., VIYANANT, V., UPATHAM, E.S., KUSAMRAN, T., CHOMPOOCHAN, T., THAMMASART, S. AND PRASITIRAT, P. Fasciola gigantica: identification of adult antigens, their tissue sources and possible origins. J Sci Soc Thailand, 22: 143-162, 1996.